About Supersymmetric Hydrogen

Robin Schneider [12]

supervised by
Prof. Yuji Tachikawa[2]
Prof. Guido Festuccia[1]

August 31, 2017

[1]Theoretical Physics - Uppsala University
[2]Kavli IPMU - The University of Tokyo

Abstract

The energy levels of atomic hydrogen obey an n^2 degeneracy at $\mathcal{O}(\alpha^2)$. It is a consequence of an $\mathfrak{so}(4)$ symmetry, which is broken by relativistic effects such as the fine or hyperfine structure, which have an explicit angular momentum and spin dependence at higher order in α.

The energy spectra of hydrogenlike bound states with underlying supersymmetry show some interesting properties. For example, in a theory with $\mathcal{N}=1$, the hyperfine splitting disappears and the spectrum is described by supermultiplets with energies solely determined by the super spin j and main quantum number n [1, 2]. Adding more supercharges appears to simplify the spectrum even more. For a given excitation V_l, the spectrum is then described by a single multiplet for which the energy depends only on the angular momentum l and n.

In 2015 Caron-Huot and Henn showed that hydrogenlike bound states in $\mathcal{N} = 4$ super Yang Mills theory preserve the n^2 degeneracy of hydrogen for relativistic corrections up to $\mathcal{O}(\alpha^3)$ [3]. Their investigations are based on the dual super conformal symmetry of $\mathcal{N} = 4$ super Yang Mills. It is expected that this result also holds for higher orders in α.

The goal of this thesis is to classify the different energy spectra of supersymmetric hydrogen, and then reproduce the results found in [3] by means of conventional quantum field theory. Unfortunately, it turns out that the techniques used for hydrogen in (S)QED are not suitable to determine the energy corrections in a model where the photon has a massless scalar superpartner. It can, however, be shown that the $\mathfrak{so}(4)$ symmetry is preserved, at least in the heavy proton limit, where $m_p \to \infty$ with the help of relativistic quantum mechanics.

Abstrakt på svenska

Energinivåerna i väteatomen följer en n^2 degeneration vid $\mathcal{O}(\alpha^2)$. Detta är en följd av en $\mathfrak{so}(4)$-symmetri vilken är bruten av relativistiska effekter som fin- och hyperfinstrukturen vilka i sin tur beror explicit på rörelsemängdsmoment och spinn vid högre ordning i α.

Energispektrumen i väteliknande bundna tillstånd med underliggande supersymmetri uppvisar vissa intressanta egenskaper. Till exempel: i en teori med $\mathcal{N}=1$ försvinner hyperfinstrukturen och spektrumet beskrivs av supermultipletter vars energier bestäms av enbart superspinn j, och huvudkvanttalet n [1, 2]. Tillägg av fler superladdningar verkar förenkla spektrumet ytterligare. För en given excitation V_l beskrivs spektrumet av en enda multiplett där energin endast beror på rörelsemängdsmomentet l och n.

År 2015 visade Caron-Huot och Henn att väteliknande bundna tillstånd i super-Yang-Mills-teori med $\mathcal{N} = 4$ bevarar n^2-degenerationen från väte för relativistiska korrektioner upp till $\mathcal{O}(\alpha^3)$ [3]. Deras undersökningar är baserade på denna duala superkonforma symmetrin i $\mathcal{N} = 4$ super-Yang-Mills. Man förväntar sig att detta resultat håller även för högre ordningar i α.

Målet med denna uppsats är att klassificera de olika energispektrumen hos supersymmetriskt väte och att därefter reproducera resultaten från [3] genom att använda konventionell kvantfältteori. Olyckligtvis visar det sig att teknikerna som används för väte i (S)QED inte lämpar sig för att bestämma energikorrektioner i en modell där fotonen har en masslös skalär superpartner. Man kan dock visa att $\mathfrak{so}(4)$-symmetrin är bevarad med hjälp av relativistisk kvantmekanik, åtminstone i gränsvärdet där protonen är tung, där $m_p \to \infty$.

Contents

Chapter 1

Introduction

The hydrogen atom is one of the best studied systems in theoretical and experimental physics. It has a rich history of new discoveries and progress in both fields. The beginning of modern atomic hydrogen physics was marked by Bohr and Rutherford, who abandoned the classical theories and postulated in 1913 that the electron moves on quantized orbits around the proton. From that assumption, they deduced a n^2 energy dependence at $\mathcal{O}(\alpha^2)$ [4]. The same n^2 degeneracy was later derived by Pauli in 1922 when investigating the symmetries of a central potential, i.e. conservation of angular momentum and Runge-Lenz vector [5]. Solving the time independent Schroedinger equation allows to give more precise corrections of the energy levels at $\mathcal{O}(\alpha^4)$ but failed to predict the proper contribution of the fine structure [6]. This was achieved by incorporating the spin dependence in terms of the relativistic Dirac equation in 1928 [7]. One year later, Fermi explained the hyperfine splitting by introducing a spin-spin contact interaction [8]. The next big theoretical step was made by Bethe, who calculated the Lamb shift, which had been found in 1947 [9], in terms of radiative corrections [10]. Even though the hydrogen atom has been studied for such a long time, there is still an active community involved in its research. Those activities include mostly the better measurement of its energy levels, and with it, more accurate theoretical predictions of their splitting [11].

In theoretical physics there has recently been a new interest in investigating hydrogenlike bound states with different underlying supersymmetries. The concept of supersymmetry (SUSY) was introduced in the 70's as an extension to the Poincaré algebra. In a supersymmetric theory every particle has so called superpartners. These partners share the same mass and charge; additionally there has to be an equal number of fermionic and bosonic degrees of freedom. SUSY was proposed in order to solve several theoretical problems and weaknesses, for example the hierarchy problem and the unification of electromagnetic weak and strong force. Furthermore, SUSY offers reasonable candidates for dark matter particles. The Minimal Supersymmetric Standard Model (MSSM) is a widely accepted extension of the standard model, which provides a solution to previously mentioned issues. Since no superpartners have been observed so far, SUSY must be broken at low energies. The search for these particles in particle colliders such as CERN is ongoing [12].

Supersymmetric bound states were investigated for the first time in 1981 by Buchmueller, Love and Peccei [13]. They analyzed the ground state energy of

superpositronium in $\mathcal{N} = 1$ and found a lack of hyperfine structure. The different particle bound state representations can be categorized in a para- and an ortho-supermultiplet. This research was extended by Di Vecchia and Schuchhardt to $\mathcal{N} = 2$, who discovered that the splitting between both supermultiplets disappears [14] and the ground state is then described by a single large multiplet.

In 2010, Herzog and Klose, [1] and independently Rube and Wacker, [2] investigated the full energy spectrum of supersymmetric hydrogen. They confirmed the lack of hyperfine splitting found earlier for superpositronium, and derived an easy expression for the energy of every supermultiplet. Their energy only depends on the superspin j and the main quantum number n. The ground state contains two supermultiplets with $j = 0$ and one with $j = \frac{1}{2}$. For a given angular momentum $l > 0$ there are four supermultiplets with $j = l \pm \frac{1}{2}, 2 \cdot l$.

Herzog and Klose motivated their work by the gauge/gravity duality, which allows us to map problems from field theories to string theory. AdS/CFT correspondence was proposed in 1997 by Juan Maldacena [15]. One common example of this mapping is the duality between $\mathcal{N} = 4$ super Yang Mills theory and Type IIb string theory.

It so happens that in 2015 Caron-Huot and Henn published a paper about hydrogenlike bound states in $\mathcal{N} = 4$ super Yang Mills [3]. They made the fascinating observation that the $\mathfrak{so}(4)$ symmetry, which is broken for (supersymmetric) hydrogen by relativistic corrections, appears to be preserved in the Coulomb phase of $\mathcal{N} = 4$ super Yang Mills theory. In their paper, the $2 \to 2$ massive vector boson scattering amplitude is analyzed by making use of the dual super conformal symmetry properties. The bound state energy is determined from its poles.

The outline of this thesis is as follows: In chapter 2, I will, 1.) review the physics of atomic hydrogen in terms of its symmetries and then 2.) analyze its energy spectrum up to $\mathcal{O}(\alpha^4)$ using Feynman diagrams. In chapter 3, the energy spectrum of supersymmetric hydrogen is derived in terms of its supermultiplets. The calculations of the relativistic energy corrections are outlined and the main results of [1] stated. Using the same field theoretical approach as in the earlier chapters, I will calculate the energy corrections of hydrogen in $\mathcal{N} = 4$ super Yang Mills in chapter 4. Unfortunately, it turns out that these calculations cannot confirm the n^2 degeneracy found in [3]. This can be explained by several shortcomings, which make the field theoretical treatment using only tree level diagrams incomplete. They are discussed in chapter 5. Making use of relativistic quantum mechanics, I will show that in an equivalent model with the heavy proton limit the $\mathfrak{so}(4)$ symmetry is preserved up to $\mathcal{O}(\alpha^4)$. This work forms the basis of a soon to be published paper [16]. The last chapter will give an outlook to future studies using effective field theories.

Chapter 2

Theory

It is a well known fact that the n^2 degeneracy of hydrogen is the result of a preserved $\mathfrak{so}(4)$ symmetry. This was shown for the first time by W. Pauli in 1922, [5] who investigated the conserved quantities of angular momentum and Runge-Lenz vector. The $\mathfrak{so}(4)$ symmetry is broken by relativistic effects at $\mathcal{O}(\alpha^4)$. The energy corrections are found from the Dirac equation with the help of quantum electro dynamics. In this chapter, I will first derive the n^2 degeneracy and then determine all operators which contribute to the energy at $\mathcal{O}(\alpha^4)$ with the help of Feynman diagrams; this includes the commonly known fine and hyperfine structure.

Within the framework of this thesis, I will work in natural units $\hbar = c = \epsilon_0 = 1$ and neglect the composite particle effects of the proton, hence, treat it as a fermionic point particle like the electron. In the literature, such a system is usually referred to as muonic hydrogen.

Furthermore, I will follow the notation and conventions of indices, particles and superfields introduced by Wess and Bagger [17]. Finally, I want to mention that I am mainly interested in effects up to $\mathcal{O}(\alpha^4)$ but will occasionally comment on radiative corrections at higher order in α such as the Lamb shift.

2.1 Hydrogen and group theory

An extensive discussion about hydrogen and group theory is given in [18]. This section contains only a short derivation of the degenerate energy levels (a review of which can be found in nearly every modern text book of quantum mechanics e.g. [19]) based on W. Pauli's work. The following Hamiltonian

$$\mathcal{H} = \frac{\vec{p}^2}{2\mu} - \frac{\alpha}{r} \tag{2.1.1}$$

describes a central potential where $\mu = (1/m_\mathrm{e} + 1/m_\mathrm{p})$ is the reduced mass, and α the fine structure constant. This potential obeys a $\mathfrak{so}(3)$ symmetry spanned by the angular momentum operators

$$[L_i, L_j] = i\epsilon_{ij}^k L_k \ . \tag{2.1.2}$$

The angular momentum is a conserved quantity. In addition, there is another conserved quantity which has been known for a long time. The quantum mechanical hermitian Runge-Lenz vector

$$\vec{M} = \frac{1}{2\mu}\big(\vec{p}\times\vec{L} - \vec{L}\times\vec{p}\big) - \alpha\frac{\vec{r}}{r} \tag{2.1.3a}$$

$$\vec{M}^2 = \frac{2}{\mu}\mathcal{H}\big(\vec{L}^2+1\big) + \alpha^2 \tag{2.1.3b}$$

$$[M_i, M_j] = -\frac{2i}{\mu}\epsilon_{ij}^k \mathcal{H} L_k \tag{2.1.3c}$$

is responsible for keeping the rotating electron on a closed disk. Hence, the full symmetry of the Hamiltonian is described by

$$\mathfrak{so}(3)\otimes\mathfrak{so}(3) = \mathfrak{so}(4)\ . \tag{2.1.4}$$

This can be easily shown by constructing the combined algebra. Both Runge-Lenz vector and angular momentum commute with the Hamiltonian

$$[\mathcal{H}, M] = 0 \tag{2.1.5a}$$

$$[\mathcal{H}, L] = 0\ . \tag{2.1.5b}$$

After appropriate rescaling, $\hat{\mathrm{M}} \equiv i\sqrt{\mu/(2E)}\,\vec{M}$, one finds the algebra

$$[L_i, L_j] = i\epsilon_{ij}^k L_k \tag{2.1.6a}$$

$$[\hat{\mathrm{M}}_i, L_j] = i\epsilon_{ij}^k \hat{\mathrm{M}}_k \tag{2.1.6b}$$

$$[\hat{\mathrm{M}}_i, \hat{\mathrm{M}}_j] = i\epsilon_{ij}^k L_k\ . \tag{2.1.6c}$$

Combining $\vec{L}$ and $\hat{\mathrm{M}}$ results in two commuting 'angular momentum' operators, which satisfy

$$A^2 = \left[\frac{\vec{L}-\hat{\mathrm{M}}}{2}\right]^2 = j_1(j_1+1) \tag{2.1.7a}$$

$$B^2 = \left[\frac{\vec{L}+\hat{\mathrm{M}}}{2}\right]^2 = j_2(j_2+1)\ . \tag{2.1.7b}$$

From $\vec{L}\cdot\hat{\mathrm{M}} = 0$ follows that $j_1 = j_2 = j = 0, \frac{1}{2}, 1, ..\ .$ Now acting on a bound state $|\psi\rangle$ with

$$\begin{aligned} A^2 + B^2\,|\psi\rangle = 2j(j+1)\,|\psi\rangle &= \frac{1}{2}\big(\vec{L}^2 - \hat{\mathrm{M}}^2\big)\,|\psi\rangle \\ &= \frac{1}{2}\big(-1 - \frac{\mu}{2E}\alpha^2\big)\,|\psi\rangle \end{aligned} \tag{2.1.8}$$

gives the energy relation

$$E = -\frac{\alpha^2\mu}{2n^2} \tag{2.1.9}$$

where $n^2 = (2j+1)^2$. One finds the well known n^2 degenerate energy spectrum following from the preservation of the $\mathfrak{so}(4)$ symmetry.

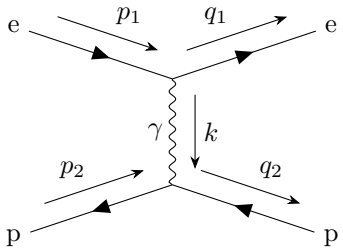

Figure 2.1: The tree level scattering diagram of an electron and a proton. The particles form a bound state, the hydrogen atom, via exchange of a photon.

2.2 Hydrogen and QED

The energy spectrum at $\mathcal{O}(\alpha^4)$ is determined by including additional effects such as the spin-orbit and spin-spin coupling, but also relativistic corrections to the momentum. They can all be obtained when starting from the Lagrangian describing the usual Dirac equation

$$\mathcal{L} = \bar{\psi}_{\mathrm{e}}(i\not{\mathcal{D}} + m_{\mathrm{e}})\psi_{\mathrm{e}} + \bar{\psi}_{\mathrm{p}}(i\not{\mathcal{D}} + m_{\mathrm{p}})\psi_{\mathrm{p}} \tag{2.2.1}$$

where $\mathcal{D}$ is the Abelian covariant derivative and ψ the Dirac spinors of electron and antiproton. The energy levels of the proton-electron bound state are determined from the potential, which is connected to the scattering amplitude $\mathcal{M}$ in the non relativistic limit via the Born approximation [20]

$$\mathcal{M}_{\mathrm{NR}} = -\langle q|\, V\, |p\rangle \ . \tag{2.2.2}$$

Hence, in order to find the Hamiltonian, one has to take the Fourier transformation of the scattering amplitude described by the Feynman diagram in figure 2.1. The Fourier transformation of $\mathcal{M}_{\mathrm{NR}}$ is performed with respect to $(\vec{p} - \vec{q}) = \vec{k} \to r$ while the momentum $\vec{p}$ is kept as a variable.

Here the different normalizations between quantum mechanics $\langle q|\, \mathbf{1}\, |p\rangle = \delta^3(\vec{p} - \vec{q})$ and quantum field theory $\langle q|\, \mathbf{1}\, |p\rangle = \sqrt{2E}\delta^3(\vec{p} - \vec{q})$ have to be taken into account

$$\mathcal{M}_{\mathrm{NR}} = \frac{\mathcal{M}}{4\big[(m_{\mathrm{e}}^2 + \vec{p}^2)(m_{\mathrm{e}}^2 + \vec{q}^2)(m_{\mathrm{p}}^2 + \vec{p}^2)(m_{\mathrm{p}}^2 + \vec{p}^2)\big]^{\frac{1}{4}}} \ . \tag{2.2.3}$$

The tree level amplitude from figure 2.1 is determined by using the conventional Feynman rules of QED

$$\mathcal{M} = (-ig)^2 \bar{u}_{\mathrm{e}}(q_1)\gamma^m u_{\mathrm{e}}(p_1)(-i)\left[\frac{\eta_{mn}}{k^2} - (1-\xi)\frac{k_m k_n}{k^4}\right]\bar{v}_{\mathrm{p}}(p_2)\gamma^n v_{\mathrm{p}}(q_2) \tag{2.2.4}$$

where the gauge dependence is kept explicit. It is most easily calculated in the center of mass frame

$$p_1 = \left(\sqrt{\vec{p}^2 + m_{\mathrm{e}}^2}\ ,\ \vec{p}\right), \qquad q_1 = \left(\sqrt{\vec{q}^2 + m_{\mathrm{e}}^2}\ ,\ \vec{q}\right), \tag{2.2.5a}$$

$$p_2 = \left(\sqrt{\vec{p}^2 + m_{\mathrm{p}}^2}\ ,\ -\vec{p}\right), \qquad q_2 = \left(\sqrt{\vec{q}^2 + m_{\mathrm{p}}^2}\ ,\ -\vec{q}\right). \tag{2.2.5b}$$

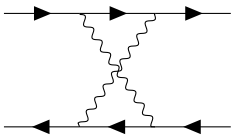

Figure 2.2: One loop cross photon scattering diagram with leading energy contributions to the bound state of $\mathcal{O}(\alpha^4)$. In Coulomb gauge, however, the leading contribution cancels to zero.

Borrowing the notation from [1] the Dirac spinors are

$$u_{\mathrm{e}}(p_1) = \begin{pmatrix} \sqrt{\sigma \cdot p_1}\xi_{\mathrm{e}} \\ \sqrt{\bar{\sigma} \cdot p_1}\xi_{\mathrm{e}} \end{pmatrix}, \quad \bar{u}_{\mathrm{e}}(q_1) = \left(-\sqrt{\bar{\sigma} \cdot q_1}\xi_{\mathrm{e}}^\dagger \, , \, -\sqrt{\sigma \cdot q_1}\xi_{\mathrm{e}}^\dagger\right), \tag{2.2.6a}$$

$$v_{\mathrm{p}}(q_2) = \begin{pmatrix} \sqrt{\sigma \cdot q_2}\eta_{\mathrm{p}} \\ -\sqrt{\bar{\sigma} \cdot q_2}\eta_{\mathrm{p}} \end{pmatrix}, \quad \bar{v}_{\mathrm{p}}(p_2) = \left(\sqrt{\bar{\sigma} \cdot p_2}\eta_{\mathrm{p}}^\dagger \, , \, -\sqrt{\sigma \cdot p_2}\eta_{\mathrm{p}}^\dagger\right). \tag{2.2.6b}$$

Using the identities A.1.5 and A.1.6a, A.1.6b, A.1.6c the amplitude becomes [1],

$$\begin{aligned} i\mathcal{M} \simeq \xi_{\mathrm{e}\,\mathrm{o}}^\dagger \eta_{\mathrm{p}\,\mathrm{i}}^\dagger \frac{4m_{\mathrm{e}}m_{\mathrm{p}}g^2}{(\vec{p}-\vec{q})^2}\Bigg[1 + \frac{1}{8}(\vec{p}+\vec{q})^2\left(\frac{1}{m_{\mathrm{e}}} + \frac{1}{m_{\mathrm{p}}}\right)^2 - \frac{(1-\xi)}{4m_{\mathrm{e}}m_{\mathrm{p}}}\frac{((\vec{p}^2-\vec{q}^2))^2}{(\vec{p}-\vec{q})^2} \\ - \frac{i}{2}(\vec{p}\times\vec{q})\cdot\vec{\sigma}_{\mathrm{e}}\left(\frac{1}{2m_{\mathrm{e}}^2} + \frac{1}{m_{\mathrm{e}}m_{\mathrm{p}}}\right) + \frac{i}{2}(\vec{p}\times\vec{q})\cdot\vec{\sigma}_{\mathrm{p}}\left(\frac{1}{2m_{\mathrm{p}}^2} + \frac{1}{m_{\mathrm{e}}m_{\mathrm{p}}}\right) \\ + \frac{1}{4m_{\mathrm{e}}m_{\mathrm{p}}}(\vec{p}-\vec{q})^2\vec{\sigma}_{\mathrm{e}}\cdot\vec{\sigma}_{\mathrm{p}} - \frac{1}{4m_{\mathrm{e}}m_{\mathrm{p}}}(\vec{p}-\vec{q})\cdot\vec{\sigma}_{\mathrm{e}}(\vec{p}-\vec{q})\cdot\vec{\sigma}_{\mathrm{p}}\Bigg]\xi_{\mathrm{e}\,\mathrm{i}}\eta_{\mathrm{p}\,\mathrm{o}}\,, \end{aligned} \tag{2.2.7}$$

Here, the non relativistic approximation $p^0 \approx m + \frac{\vec{p}^2}{2m}$ was used, omitting terms of momenta $\alpha\vec{p}^4$ which scale with at least $\mathcal{O}(\alpha^5)$. I will henceforth use Coulomb gauge with $\xi = 0$. In any other gauge one loop diagrams coming from cross photon scattering as in figure 2.2 have to be considered at $\mathcal{O}(\alpha^4)$ in bound state energy [21]. This is discussed in more detail in section 5.2.

According to 2.2.3, when going from $\mathcal{M} \to \mathcal{M}_{\mathrm{NR}}$ the amplitude receives many corrections. However, only the ones coming from the normalization of the Coulomb potential, the first term in 2.2.7, are of $\mathcal{O}(\alpha^4)$

$$\Delta\mathcal{M} = -(\vec{p}^2 + \vec{q}^2)\left(\frac{1}{4m_{\mathrm{e}}^2} + \frac{1}{4m_{\mathrm{p}}^2}\right). \tag{2.2.8}$$

After transforming the antispinors to spinors with $\eta = i\sigma^2\xi^*$, some massaging (use identity A.1.7) and a subsequent Fourier transformation, one finds the potential

$$\begin{aligned} V(\vec{r},\vec{p}) = \alpha\Bigg[-\frac{1}{r} - \frac{1}{m_{\mathrm{e}}m_{\mathrm{p}}}\left(\frac{\vec{p}^2}{2r} + \frac{(\vec{r}\cdot\vec{p})^2}{2r^3} + \pi\delta^3(\vec{r})\right) + \frac{\pi}{2}\delta^3(\vec{r})\left(\frac{1}{m_{\mathrm{e}}} + \frac{1}{m_{\mathrm{p}}}\right)^2 \\ + \frac{\vec{L}\cdot\vec{S}_e}{r^3}\left(\frac{1}{2m_{\mathrm{e}}^2} + \frac{1}{m_{\mathrm{e}}m_{\mathrm{p}}}\right) + \frac{\vec{L}\cdot\vec{S}_p}{r^3}\left(\frac{1}{2m_{\mathrm{p}}^2} + \frac{1}{m_{\mathrm{e}}m_{\mathrm{p}}}\right) \\ + \frac{1}{m_{\mathrm{e}}m_{\mathrm{p}}}\left(\frac{8\pi}{3}\vec{S}_e\cdot\vec{S}_p\delta^3(\vec{r}) + \frac{3\vec{r}\cdot\vec{S}_e\vec{r}\cdot\vec{S}_P - \vec{S}_e\cdot\vec{S}_p}{r^3}\right)\Bigg]. \end{aligned} \tag{2.2.9}$$

Every operator is understood to be normal ordered. Comparing this result with the Breit potential [22, 23], one identifies the usual terms such as (i) the Coulomb potential, (ii) the orbit-orbit interaction, (iii) the Darwin term, which only contributes to s-waves, (iv) + (v) the spin-orbit interactions and (vi) the spin-spin interactions.

The energy spectrum of atomic hydrogen is then determined with perturbation theory. First, however, there is one relativistic correction which is still missing; the Hamiltonian of any quantum mechanical system is given by

$$\mathcal{H} = T + V \ . \tag{2.2.10}$$

Expanding the kinetic energy

$$\begin{aligned} T = E - M_{\text{tot}} &= \sqrt{m_{\text{e}}^2 + \vec{p}^2} + \sqrt{m_{\text{p}}^2 + \vec{p}^2} - (m_{\text{e}} + m_{\text{p}}) \\ &\simeq m_{\text{e}}\left(1 + \frac{\vec{p}^2}{2m_{\text{e}}^2} - \frac{\vec{p}^4}{8m_{\text{e}}^4}\right) + m_{\text{p}}\left(1 + \frac{\vec{p}^2}{2m_{\text{p}}^2} - \frac{\vec{p}^4}{8m_{\text{p}}^4}\right) - (m_{\text{e}} + m_{\text{p}}) \\ &= \frac{\vec{p}^2}{2}\left(\frac{1}{m_{\text{e}}} + \frac{1}{m_{\text{p}}}\right) - \frac{\vec{p}^4}{8}\left(\frac{1}{m_{\text{e}}^3} + \frac{1}{m_{\text{p}}^3}\right) \end{aligned} \tag{2.2.11}$$

gives an additional term $\propto \vec{p}^4$ scaling with $\mathcal{O}(\alpha^4)$. The full Hamiltonian becomes

$$\begin{aligned} \Rightarrow \mathcal{H} &= \frac{\vec{p}^2}{2\mu} - \frac{\vec{p}^4}{8}\left(\frac{1}{m_{\text{e}}^3} + \frac{1}{m_{\text{p}}^3}\right) + V(\vec{r}, \vec{p}) \\ &= \frac{\vec{p}^2}{2\mu} - \frac{\alpha}{r} + \mathcal{H}_{\text{int}}(\vec{r}, \vec{p}) \end{aligned} \tag{2.2.12}$$

where in the last line I decomposed it into an interaction part and the usual Coulomb potential. In first order degenerate perturbation theory, the energy shifts are determined by taking the expectation value (EV)

$$\delta E_{nl} = \langle \psi_{nl} | \, H_{\text{int}} \, | \psi_{nl} \rangle \ . \tag{2.2.13}$$

EVs of the different operators can be found in the appendix A.2. Energy corrections scaling with $\sim \mu\alpha^4$, such as the electron spin-orbit, the Darwin and the $\vec{p}^4$ momentum operator, are often referred to as fine structure

$$\delta E_{nj}^{\text{fine}} = -\frac{\mu\alpha^4}{n^4}\left[\frac{n}{2j+1} - \frac{3}{8}\right] , \tag{2.2.14}$$

where $j = l \pm \frac{1}{2}$ is the total angular momentum. The explicit j dependence breaks the n^2 degeneracy, and with it the $\mathfrak{so}(4)$ symmetry. Hyperfine structure corrections are all those terms $\propto \mu\alpha^4 m_{\text{e}}/m_{\text{p}}$. Due to their l and spin dependence, they also break the n^2 degeneracy. The term hyperfine splitting is commonly used to describe the splitting of the s-waves into singlet and triplet, breaking the degeneracy of the ground state. This is a consequence of the spin-spin interactions in the last line of equation 2.2.9, which gives different values depending on the alignment of the two spins; i.e. the ground state splits into

$$\begin{cases} \text{Singlet:} & \frac{1}{\sqrt{2}}\big(\,|\uparrow\downarrow\rangle - |\downarrow\uparrow\rangle\,\big) & \Delta E \propto -3\alpha^4\mu\frac{m_{\text{e}}}{m_{\text{p}}} \\ \text{Triplet:} & \frac{1}{\sqrt{2}}\big(\,|\uparrow\downarrow\rangle + |\downarrow\uparrow\rangle\,\big) \ , \ |\uparrow\uparrow\rangle \ , \ |\downarrow\downarrow\rangle & \Delta E \propto \alpha^4\mu\frac{m_{\text{e}}}{m_{\text{p}}} \ . \end{cases} \tag{2.2.15}$$

Compared to the fine structure, its magnitude is significantly smaller, as it is suppressed by the proton mass $\sim 1/2000$.

In next leading order of α one finds the Lamb shift $\mathcal{O}(\alpha^5 \log(\alpha))$ coming from radiative corrections to the bound state. Even though it comes with a higher order in α, its contribution is significantly larger than the hyperfine splitting. It is obtained by calculating the loop diagrams describing corrections to the vertices, and the vacuum polarization. For a full treatment of (hyper-)fine structure and Lamb shift, Quantum Field Theory by Itzykson and Zuber is a valuable resource [24].

Chapter 3

Supersymmetric Hydrogen

In this chapter I will provide a review of $\mathcal{N}=1$ supersymmetric hydrogen. The focus will be on the structure of the energy spectrum in terms of its supermultiplets. The energy shifts between these supermultiplets have to be explicitly calculated from the Hamiltonian. This was done independently by Herzog and Klose, [1] and Rube and Wacker [2]. I will also briefly comment on an extension to $\mathcal{N}=2$. The only explicit $\mathcal{N}=2$ SQED bound state analysis using Feynman diagrams was performed by Di Vecchia and Schuchhardt in 1985 for the ground state of superpositronium [14].

The Lagrangian of supersymmetric hydrogen in terms of $\mathcal{N}=1$ superfields is

$$\begin{aligned}\mathcal{L} &= \mathcal{L}_{\text{gauge}} + \mathcal{L}_{\text{matter}} \\ &= \left[\int \mathrm{d}^2\theta\, \mathcal{W}\mathcal{W} + \text{h.c.}\right] + \left[\int \mathrm{d}^4\theta \big(\Phi_{\text{e}+}^\dagger \mathrm{e}^{2gV}\Phi_{\text{e}+} + \Phi_{\text{e}-}^\dagger \mathrm{e}^{-2gV}\Phi_{\text{e}-}\big)\right. \\ &\quad \left. + \int \mathrm{d}^2\theta m_{\text{e}}(\Phi_{\text{e}+}\Phi_{\text{e}-} + \Phi_{\text{e}+}^\dagger\Phi_{\text{e}-}^\dagger) + \text{proton terms}\right].\end{aligned} \tag{3.0.1}$$

It is build from four massive chiral fields ($\Phi_{\text{e/p}\pm}$) and one massless vector field (V). Each chiral field contains a Weyl spinor and a complex scalar. Two of these Weyl spinors then combine and form the Dirac spinors of electron and antiproton. In total, the particle spectrum is that of four complex scalars ($\phi_{\text{e/p}\pm}$), one electron (ψ_{e}) and the antiproton (ψ_{p}). The vector field has the role of the gauge field. It is conventional to use Wess-Zumino gauge, such that its particle spectrum is given by a massless vector boson, the photon γ, and its superparticle the gaugino, a massless Majorana fermion λ. $\mathcal{W}$ is the Abelian superfield strength. The gaugino couples a Weyl spinor to its complex scalar, and is therefore responsible for mixing between different bound states.

3.1 Energy spectrum

A rigorous analysis of the energy and particle spectrum in terms of symmetries can be found in [2] [25]. The review in the next two sections follows closely [1] and states their main results.

At leading order the bound states are n^2 degenerate as a consequence of the Coulomb potential coming from the photon exchange. However, at next to

leading order, the bound states receive relativistic and spin dependent energy corrections. The bound state spectrum, in terms of its superparticles, transforms as

$$\mathcal{S} = (\Phi_{\mathrm{e}+} \oplus \Phi_{\mathrm{e}-}) \otimes (\Phi_{\mathrm{p}+} \oplus \Phi_{\mathrm{p}-}) \,. \tag{3.1.1}$$

For the ground state with $l = 0$ there are in total eight bosonic

$$\begin{cases} \text{Fermion-Fermion:} & |\uparrow\uparrow\rangle \,,\ |\uparrow\downarrow\rangle \,,\ |\downarrow\uparrow\rangle \,,\ |\downarrow\downarrow\rangle \\ \text{Scalar-Scalar:} & |{+}{+}\rangle \,,\ |{-}{+}\rangle \,,\ |{+}{-}\rangle \,,\ |{-}{-}\rangle \end{cases} \tag{3.1.2}$$

and eight fermionic

$$\begin{cases} \text{Fermion-Scalar:} & |\uparrow +\rangle \,,\ |\uparrow -\rangle \,,\ |\downarrow +\rangle \,,\ |\downarrow -\rangle \\ \text{Scalar-Fermion:} & |+\uparrow\rangle \,,\ |-\uparrow\rangle \,,\ |+\downarrow\rangle \,,\ |-\downarrow\rangle \end{cases} \tag{3.1.3}$$

possible bound state. The total 16 degrees of freedom are matched by two massive multiplets and one vector multiplet built from a Clifford vacuum Ω_j

λ	$\mathcal{S}$	$2 \cdot \Omega_0$	$\Omega_{\frac{1}{2}}$
-1	1	0	1
$-\frac{1}{2}$	4	$1+1$	2
0	6	$2+2$	$1+1$
$\frac{1}{2}$	4	$1+1$	2
1	1	0	1

where λ is the helicity of a given state. Each multiplet Ω_j can be decomposed into $2j+1$ dimensional representations V_j of $\mathfrak{so}(3)$.

$$\Omega_j = V_{j-\frac{1}{2}} \oplus 2 \cdot V_j \oplus V_{j+\frac{1}{2}} \tag{3.1.4}$$

The symmetries of the Lagrangian put further constraints on the energy spectrum. $\mathrm{U}(1)_R$-symmetry and parity act on a given superparticle with

$$\mathcal{P}\Phi_\pm = \Phi_\mp \qquad R(\alpha)\Phi_\pm = \mathrm{e}^{\pm i\alpha}\Phi_\pm \,. \tag{3.1.5}$$

Hence, parity and a $R(\alpha)$ transformation do not commute; they combine as a semiproduct with $\mathrm{U}(1)_R \rtimes \mathbb{Z}_2 \cong \mathrm{O}(2)_R$. The two Ω_0 multiplets sit in a doublet of $\mathrm{O}(2)_R$ and share common eigenenergies while $\Omega_{\frac{1}{2}}$ already forms a doublet with its CPT conjugate.

For excited states, it follows from

$$V_l \otimes V_j = V_{|l-j|} \oplus \ldots \oplus V_{|l+j|} \tag{3.1.6}$$

where both and V_l and V_j are representations of $\mathfrak{so}(3)$ and 3.1.4 that

$$V_l \otimes \Omega_j = \Omega_{|l-j|} \oplus \ldots \oplus \Omega_{|l+j|} \,. \tag{3.1.7}$$

Hence, the energy spectrum for a given l decomposes as,

$$V_l \otimes (\Omega_0 \oplus \Omega_0 \oplus \Omega_{\frac{1}{2}}) = \Omega_{l-\frac{1}{2}} \oplus \Omega_l \oplus \Omega_l \oplus \Omega_{l+\frac{1}{2}} \,. \tag{3.1.8}$$

In summary, the energy spectrum for arbitrary l is expected to look as presented in figure 3.4. Surprisingly, there is no energy shift between the multiplets $\Omega_{l+\frac{1}{2}}$ and $\Omega_{l+1-\frac{1}{2}}$. This accidental degeneracy, however, has to be explicitly calculated.

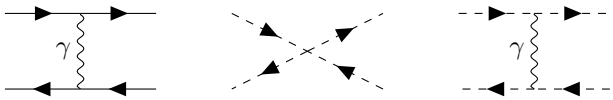

Figure 3.1: The three tree level Feynman diagrams describing the eight bosonic bound states of a $\mathcal{N} = 1$ supersymmetric hydrogen model. The first diagram shows the four fermion-fermion bound states, while second and third describe the four different scalar-scalar bound states.

Figure 3.2: The four tree level Feynman diagrams describing the mixing between bosonic i) + ii) and fermionic iii) + iv) bound states of a $\mathcal{N} = 1$ supersymmetric hydrogen model.

3.2 Energy splitting

In order to determine the energies of the supermultiplets, one has to find the Hamiltonian. This is a familiar task from section 2.2 where the Hamiltonian for atomic hydrogen was calculated. The relevant Feynman diagrams of the eight bosonic bound states are presented in figure 3.1. The amplitudes of the second and third diagram representing the scalar-scalar bound states are straightforwardly calculated. Their resulting potentials contain the Coulomb attraction, the orbit-orbit interaction and the Darwin correction.

As a consequence of supersymmetry, the different bosonic bound states can mix with each other. They do this by exchanging a gaugino, as shown in figure 3.2. From the first two diagrams, one derives the potential

$$V_{\text{mix}} = -\frac{g^2}{4\pi}\xi_{\text{p}}^{\text{T}}\Bigg[-\frac{i}{2\sqrt{m_{\text{e}}m_{\text{p}}}}\frac{\vec{r}\cdot\bar{\sigma}}{r^3} \pm \frac{\pi}{2}\frac{m_{\text{p}}-m_{\text{e}}}{(m_{\text{e}}m_{\text{p}})^{\frac{3}{2}}}\delta^3(\vec{r}) \pm \frac{1}{4}\frac{m_{\text{p}}+m_{\text{e}}}{(m_{\text{e}}m_{\text{p}})^{\frac{3}{2}}}\frac{\vec{L}\cdot\vec{\sigma}}{r^3}\Bigg]\xi_{\text{e}} \ . \tag{3.2.1}$$

In contrast to other corrections, the first term scales with $\mathcal{O}(\alpha^3)$. However, it turns out that

$$\langle\frac{\vec{r}}{r^3}\rangle = 0 \tag{3.2.2}$$

and V_{mix} therefore contributes only with second order perturbation theory

$$\delta E_2 = \sum_i \frac{|\langle\psi_i| H_{\text{int}} |\psi_n\rangle|^2}{E_n - E_i} \ . \tag{3.2.3}$$

The energy correction is then proportional to $\propto \alpha^4$. The integral $\langle\psi_i| H_{\text{int}} |\psi_n\rangle$ is solved with the help of Schwingers solution to the Coulomb Green function [26]. Having determined all energy corrections, one can rewrite the Hamiltonian as a 8x8 matrix spanned by the bound states, given in 3.1.2. From a first guess, this should only be possible for s-waves as one expects states in higher orbitals to mix for different values of l. However, it turns out that neither second order

Figure 3.3: The two tree level diagrams describing the eight fermionic bound states of a $\mathcal{N} = 1$ supersymmetric hydrogen model. Each diagram represents the four different bound states arising from a coupling between one fermion and two complex scalar.

perturbation theory nor the spin-spin interactions mix states of different n and l. The analysis of the eight fermionic bound states follows the same reasoning. In figure 3.3 are the two relevant tree level diagrams to determine the fermionic Hamiltonian, while the third and fourth diagram in figure 3.2 show the mixing contributions.

Before calculating the eigenvalues of the Hamiltonians, it is useful to split them into two parts

$$\mathcal{H} = \mathcal{H}_{\text{common}} + \mathcal{H}_{\text{specific}} \tag{3.2.4}$$

where the common Hamiltonian includes the Coulomb attraction, the orbit-orbit interaction and the relativistic correction, which are the same for all bound states. Its energy correction is

$$\delta E_{\text{common}}(nl) = -\frac{\mu\alpha^2}{2n^2} - \frac{\mu\alpha^4}{n^4}\left[\frac{n}{2l+1} - \frac{3}{8} + \frac{\mu}{8m_{\text{e}}m_{\text{p}}}\right]. \tag{3.2.5}$$

Then, $\mathcal{H}_{\text{specific}}$ gives the splitting between the supermultiplets. Since the Darwin term only contributes to s-waves, while spin-orbit interactions are only nonzero for $l \neq 0$, the cases $l = 0$ and $l > 0$ are treated separately.

Beginning with the ground state $l = 0$, one finds two different eigenvalues, each having four eigenstates for bosonic and fermionic bound states

$$\begin{cases} \Delta E_1 = 0 \\ \Delta E_2 = \frac{\mu\alpha^4}{2n^3}\ . \end{cases} \tag{3.2.6}$$

The $2 \cdot E_1$ eigenvalues belong to the $2 \cdot \Omega_0$ super multiplets while the $2 \cdot E_2$ belong to the $\Omega_{\frac{1}{2}}$ super multiplet.

In the case of a fixed $l > 0$ there are $8 \times (2l + 1)$ bosonic and $8 \times (2l + 1)$ fermionic states. To simplify the calculations, one splits the Hamiltonian into subspaces described by m_j of the total angular momentum. For bosonic bound states one has, $m_j = m_l = -l, ..., l-1, l$ with $j = l \pm 1, l$ such that the subspace becomes

$$\begin{aligned} |\psi\rangle \in \big\{ &|lm_l, \uparrow\uparrow\rangle, |lm_l, \downarrow\uparrow\rangle, |lm_l, \uparrow\downarrow\rangle, |lm_l, \downarrow\downarrow\rangle, \\ &|lm_l, ++\rangle, |lm_l, +-\rangle, |lm_l, -+\rangle, |lm_l, --\rangle \big\}. \end{aligned} \tag{3.2.7}$$

While for fermionic bound states, one uses $m_j + \frac{1}{2} = m_l = -l, .., l, l+1$ with $j = l \pm \frac{1}{2}$

$$\begin{aligned} |\psi\rangle \in \big\{ &|lm_l, \uparrow +\rangle, |lm_l, -\uparrow\rangle, |lm_l + 1, \downarrow +\rangle, |lm_l + 1, -\downarrow\rangle, \\ &|lm_l, \uparrow -\rangle, |lm_l, +\uparrow\rangle, |lm_l + 1, \downarrow -\rangle, |lm_l + 1, +\downarrow\rangle \big\}. \end{aligned} \tag{3.2.8}$$

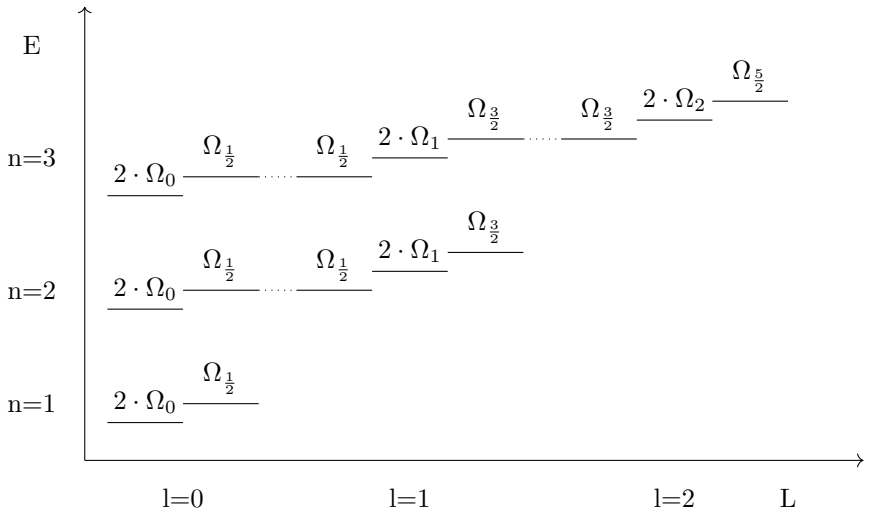

Figure 3.4: Energy spectrum of supersymmetric hydrogen. On the x-axis is the angular momentum while the y-axis shows the energy level up to $n = 3$, taken from [2]. The energy value of a given supermultiplet is determined from equation 3.2.10.

Diagonalization of $\mathcal{H}_{\text{specific}}$ yields once again the same eigenvalues for the fermionic and bosonic sector. In total, one finds three different eigenvalues for the four supermultiplets

$$\begin{cases} \Omega_{l+\frac{1}{2}}: & \Delta E_1 = \frac{\mu\alpha^4}{2(l+1)(2l+1)n^3} \\ 2\Omega_l \quad : & \Delta E_2 = 0 \\ \Omega_{l-\frac{1}{2}}: & \Delta E_3 = -\frac{\mu\alpha^4}{2l(2l+1)n^3} \end{cases}, \tag{3.2.9}$$

where ΔE_1 and ΔE_3 each have four eigenstates, and ΔE_2 occurs with $2 \cdot 4$ eigenstates. This specific l dependence makes it possible to express the energy of a given supermultiplet only in terms of its total angular momentum j (superspin)

$$E(\Omega_j) = -\frac{\mu\alpha^2}{2n^2} - \frac{\mu\alpha^4}{n^4}\left(\frac{n}{2j+1} - \frac{3}{8} + \frac{\mu^2}{8m_\text{e}m_\text{p}}\right). \tag{3.2.10}$$

Therefore multiplets, of different l but with the same j are degenerate in energy. The spectrum is presented in figure 3.4.

Particle representations

The particle representations of $V_{l\pm(\frac{1}{2},0)}$ which form the multiplets Ω_j are constructed by acting with the supercharges on a given state. In the rest frame $p = (m_\text{e} + m_\text{p}, 0, 0, 0)$ the super algebra is

$$\{Q_\alpha, \bar{Q}_{\dot{\alpha}}\} = (m_\text{e} + m_\text{p})\delta_{\alpha\dot{\alpha}} \tag{3.2.11a}$$

$$\{Q_\alpha, Q_\beta\} = \{\bar{Q}_{\dot{\alpha}}, \bar{Q}_{\dot{\beta}}\} = [Q_\alpha, \mathcal{H}] = 0\,. \tag{3.2.11b}$$

The particles transform under a supertransformation according to

$$\delta_\xi \phi_{\mathrm{e/p}+} = \pm\sqrt{m_{\mathrm{e/p}}}\xi_\alpha \psi^\alpha_{\mathrm{e/p}} \qquad \delta_\xi \phi^*_{\mathrm{e/p}-} = \pm\sqrt{m_{\mathrm{e/p}}}\bar{\xi}_{\dot\alpha}\delta^{\bar\alpha\alpha}\psi_{\mathrm{e/p}\alpha} \tag{3.2.12a}$$

$$\delta_\xi \psi_{\mathrm{e/p}\alpha} = \pm\frac{1}{2}\sqrt{m_{\mathrm{e/p}}}(\bar{\xi}_{\dot\alpha}\epsilon^{\dot\alpha}_{\alpha}\phi_{\mathrm{e/p}+} + \xi_\alpha \phi^*_{\mathrm{e/p}-}) \ . \tag{3.2.12b}$$

It is then conventional to define creation and annihilation operators that act on the Clifford vacuum

$$a^\dagger_{\dot\alpha} = \frac{\bar{Q}_{\dot\alpha}}{\sqrt{m_{\mathrm{e}}+m_{\mathrm{p}}}} \quad \rightarrow \quad a^\dagger_{\dot\alpha}\,|\lambda\rangle_{\mathrm{e/p}} = \sqrt{\frac{m_{\mathrm{e/p}}}{m_{\mathrm{e}}+m_{\mathrm{p}}}}\,|\lambda+\frac{1}{2}\rangle_{\mathrm{e/p}} \tag{3.2.13}$$

such that they satisfy

$$\{a_\alpha, a^\dagger_{\dot\alpha}\} = \delta_{\alpha\dot\alpha} \ . \tag{3.2.14}$$

The particle representations of V_j are found by acting with the creation operators on the state of lowest helicity. For example, given the multiplet Ω_0 of the ground state with $l=0$ and starting from the state $|{+}{-}\rangle$ one finds

$$\Omega_0 \begin{cases} V_0 & = |{-}{+}\rangle \\ \\ V_{\frac{1}{2}} & = a^\dagger_1\,|{-}{+}\rangle \\ & = \sqrt{\frac{m_{\mathrm{e}}}{m_{\mathrm{e}}+m_{\mathrm{p}}}}\,|{\uparrow}{+}\rangle - \sqrt{\frac{m_{\mathrm{p}}}{m_{\mathrm{e}}+m_{\mathrm{p}}}}\,|{-}{\uparrow}\rangle \\ \\ V_{\frac{1}{2}} & = a^\dagger_2\,|{-}{+}\rangle \\ & = \sqrt{\frac{m_{\mathrm{e}}}{m_{\mathrm{e}}+m_{\mathrm{p}}}}\,|{\downarrow}{+}\rangle - \sqrt{\frac{m_{\mathrm{p}}}{m_{\mathrm{e}}+m_{\mathrm{p}}}}\,|{-}{\downarrow}\rangle \\ \\ V_0 & = a^\dagger_1 a^\dagger_2\,|{-}{+}\rangle \\ & = \frac{m_{\mathrm{p}}}{m_{\mathrm{e}}+m_{\mathrm{p}}}\,|{-}{-}\rangle + \frac{m_{\mathrm{e}}}{m_{\mathrm{e}}+m_{\mathrm{p}}}\,|{+}{+}\rangle + \frac{\sqrt{m_{\mathrm{p}}m_{\mathrm{e}}}}{m_{\mathrm{e}}+m_{\mathrm{p}}}\big(\,|{\uparrow}{\downarrow}\rangle - |{\downarrow}{\uparrow}\rangle\,\big) \ . \end{cases} \tag{3.2.15}$$

For bound states with fixed $l>0$, one must consider that the supercharges carry a spin themselves. Since there is a mixing of m_j's all $4\times 4\times(2l+1)$ states for a given l-value have to be considered at the same time. The complete particle representations of excited states can be found in [1, 27].

3.3 Hydrogen in $\mathcal{N}=2$

A supersymmetric hydrogen model with $\mathcal{N}=2$ is constructed from two massive (anti-)BPS (Bogomonlyi-Prasad-Sommerfeld) multiplets, built from a Clifford vacuum Ω_0. (Anti-) BPS multiplets are supermultiplets for which half of the creation and annihilation operators are trivially satisfied. Hence, their particle representation is significantly reduced compared to long multiplets. The $\mathcal{N}=2$ BPS multiplets have the same particle representations as the two $\mathcal{N}=1$ multiplets from the previous section; they contain a Dirac fermion and two complex scalars. However, this time the two scalars transform under a $\mathfrak{su}(2)_R \simeq \mathfrak{so}(3)$ symmetry as a consequence of $\mathcal{N}=2$. The massless gauge multiplet contains an additional gaugino (η) and a complex massless scalar (π). It is

described, in terms of $\mathcal{N}=1$ superparticles, by one chiral (Π) and one vector (V) field. Summarizing this, the new Lagrangian reads [28]

$$\begin{aligned}\mathcal{L} &= \mathcal{L}_{\text{gauge}} + \mathcal{L}_{\text{matter}} \\ &= \Big[\int \mathrm{d}^2\theta\, \mathcal{W}\mathcal{W} + \text{h.c.} + \int \mathrm{d}^4\theta \Pi^\dagger \Pi\Big] + \Big[\int \mathrm{d}^4\theta \big(\Phi_{\mathrm{e}+}\mathrm{e}^{+gV}\Phi^\dagger_{\mathrm{e}+} \\ &\quad + \Phi_{e-}\mathrm{e}^{-gV}\Phi^\dagger_{e-}\big) + \int \mathrm{d}^2\theta\big[m_{\mathrm{e}}(\Phi_{\mathrm{e}+}\Phi_{\mathrm{e}-} + \Phi^\dagger_{\mathrm{e}+}\Phi^\dagger_{\mathrm{e}-}) \\ &\quad + \int \mathrm{d}^2\theta\sqrt{2}g\big[(\Phi_{\mathrm{e}+}\Phi_{\mathrm{e}-}\Pi + \Phi^\dagger_{\mathrm{e}+}\Phi^\dagger_{\mathrm{e}-}\Pi^\dagger)\big] + \text{proton terms}\Big]\,.\end{aligned} \tag{3.3.1}$$

The bound states of a BPS and anti-BPS multiplet bind together in leading order via exchange of a photon and a massless scalar. The resulting Coulomb potential is twice as strong as in usual QED and preserves the $\mathfrak{so}(4)$ symmetry. If the second multiplet were another BPS multiplet, contributions from scalar and photon exchange would exactly cancel, such that there are no existing bound states. Again, the energy spectrum receives relativistic corrections at $\mathcal{O}(\alpha^4)$. The states transform

$$\mathcal{S} = (\Phi_{\mathrm{e}}^{\text{BPS}}) \otimes (\Phi_{\mathrm{p}}^{\text{anti-BPS}}) = \Phi_{\text{BS}}^{\text{non-BPS}}\,. \tag{3.3.2}$$

The bound state is described by a massive long (vector) multiplet $\Phi^{\text{non-BPS}}$ built from a Clifford Vacuum Ω_0. A quick check reveals that it contains the same number of degrees of freedom

$$j=0 \;\rightarrow\; \left(-1, \mathbf{4}\times -\frac{1}{2}, \mathbf{6}\times 0, \mathbf{4}\times\frac{1}{2}, 1\right). \tag{3.3.3}$$

Proposition:
A product of a BPS with an anti-BPS multiplet will always transform like a non-BPS (long) multiplet.

Proof:
A SUSY algebra with $\mathcal{N}>1$ in the rest frame $p=(m_i+m_j,0,0,0)$ is given by,

$$\{Q^A_a, \bar{Q}^b_B\} = 2m\delta^b_a\delta^A_B \tag{3.3.4a}$$
$$\{Q^A_a, Q^B_b\} = \epsilon_{ab}c^{AB} \tag{3.3.4b}$$
$$\{\bar{Q}^a_A, \bar{Q}^b_B\} = \epsilon^{ab}\bar{c}_{AB} \tag{3.3.4c}$$

where I changed the $\mathfrak{su}(2)$ indices $\alpha,\dot{\alpha}$ of the antisymmetric ϵ_{ab} tensor to the little group $\mathfrak{so}(3)$ with a,b and $m=m_i+m_j$. Rewriting the central charges as $c^{AB}=cJ^{AB}$ where J^{AB} is the antisymmetric tensor of the R-symmetry and $c\in\mathbb{R}$, it is conventional to then define the creation and annihilation operators of the SUSY algebra as

$$a^A_{a\pm} \equiv \frac{1}{\sqrt{2}}\big(Q^A_a \pm J^{AB}\epsilon_{ab}\bar{Q}^b_B\big) \tag{3.3.5}$$

which satisfy the reality condition

$$(a^A_{a\pm})^\dagger = \bar{J}_{AB}\epsilon^{ab}a^B_{b\pm} \tag{3.3.6}$$

Figure 3.5: Four additional tree level diagrams of $\mathcal{N} = 2$ supersymmetric hydrogen corresponding to a massless scalar exchange.

and the anticommutation relations

$$\{a^I_{a\pm}, a^J_{b\pm}\} = (2m \pm c)J^{IJ}\epsilon_{ab} \,, \qquad \{a^I_{a\pm}, a^J_{b\mp}\} = 0 \,. \tag{3.3.7a}$$

$$\{a^I_{a\pm}, (a^J_{b\pm})^\dagger\} = (2m \pm c)\delta^I_J\delta^b_a \,. \tag{3.3.7b}$$

As a consequence of the positive finiteness of Hilbert space, one finds the BPS condition $2m \geq |c|$. For a BPS ($c_i = 2m_i$) multiplet this bound is saturated for half the operators such that,

$$\rightarrow a^A_{a-} = 0 = (a^A_{a-})^\dagger \tag{3.3.8}$$

are trivially realized. In the case of an anti-BPS ($c_j = -2m_j$) multiplet, the same holds for $a^A_{a+} = (a^A_{a+})^\dagger = 0$. Hence, when taking the product of

$$\Phi^{\text{BPS}} \otimes \Phi^{\text{anti-BPS}} = \Phi^{\text{non-BPS}} \tag{3.3.9}$$

all creation and annihilation operators of this model saturate the BPS condition $2m_{\text{BS}} > |c|$. This follows from the triangle equality, where e.g. in my case $2m_{\text{BS}} > |c_i + c_j| \Leftrightarrow |m_{\text{e}} + m_{\text{p}}| > |m_{\text{e}} - m_{\text{p}}|$ is always satisfied. The non BPS multiplet Φ_{BS} is then built from a Clifford vacuum Ω_0 and contains $2^{2\mathcal{N}-1}$ bosonic and $2^{2\mathcal{N}-1}$ fermionic states.

Hence, the energy spectrum transforms as a massive vector multiplet. This is in line with results found for positronium with $\mathcal{N} = 2$ [29]. There, the splitting between ortho- and para-mutliplet of $\mathcal{N} = 1$ superpositronium disappeared and the groundstate is described by a single massive super multiplet.

The eigenenergies of the ground state can be determined with the procedure outlined in the previous section. For that, one has to consider the additional diagrams coming from massless scalar exchanges, such as in figure 3.5, and the additional contributions of the second gaugino, with diagrams similar to those in 3.2 replacing λ with η.

The non-BPS multiplet transforms trivially under a V_l ($\mathfrak{so}(3)$) excitation, leaving a simplified energy spectrum with a single long multiplet for a given value of l and n. This can be shown by working out the combined algebra of the annihilation and creation operators, with the $\mathfrak{so}(3)$ rotations as is done in the appendix A.3

$$V_l \otimes \Phi^{\text{non-BPS}} = \Phi^{\text{non-BPS}}_l \,. \tag{3.3.10}$$

It appears now to be a simple straightforward task to determine the whole energy spectrum of the long multiplet. However, it turns out that the massless scalar exchange gives rise to a number of problems, which I will further discuss in chapter 5, since they also arise in the $\mathcal{N} = 4$ model. The corrections found in [29] for the ground state of $\mathcal{N} = 2$ superpositronium suggest an explicit l-dependence for excited bound states.

Chapter 4

$\mathcal{N} = 4$ Super Yang Mills

I started this thesis by showing that the Coulomb potential obeys a $\mathfrak{so}(3) \otimes \mathfrak{so}(3) = \mathfrak{so}(4)$ symmetry, which implies an n^2 degeneracy. Now, in 2015 Caron-Huot and Henn published a paper investigating hydrogenlike bound states in the Coulomb phase of $\mathcal{N} = 4$ super Yang Mills theory. They found that relativistic corrections up to order $\mathcal{O}(\alpha^3)$ preserve this n^2 degeneracy in the large N_c limit. Their energy corrections are

$$\delta E(n) = -\frac{\lambda^2 m}{64\pi^2 n^2} - \frac{\lambda^3 m}{64\pi^2 n^2}\left[\sum_{k=1}^{n}\left(\frac{1}{k}\right) + \log\frac{\lambda}{2\pi n} - 1 - \frac{1}{2n}\right] + \mathcal{O}(\lambda^4) \quad (4.0.1)$$

where $\lambda = g^2 N_c$ is the 't Hooft coupling.

Their calculations are based on the dual superconformal symmetry, which is equivalent to $\mathfrak{so}(4,2)$ of $\mathcal{N} = 4$ super Yang Mills theory [30]. The $2 \to 2$ vector scattering with arbitrary masses is considered where bound states appear as resonances in the process. Introducing masses to the theory appears to leave the $\mathfrak{so}(4)$ symmetry unbroken. Their results hold for strong and weak coupling.

Further calculations of massive bound states and their amplitudes have been performed for strong coupling in [31, 32, 33, 34].

The goal of this chapter is to confirm their results by calculating the leading relativistic correction with the methods introduced in the previous chapters. Starting from the $\mathcal{N} = 4$ Lagrangian, I will construct a hydrogen model containing electron and proton generation. Decomposing the bound state multiplet in its irreducible representations makes it possible to determine the relativistic $\mathcal{O}(\alpha^4)$ energy corrections, by simply considering the scalar-scalar bound state.

This chapter is based on my work in the soon to be published paper [16].

4.1 The setup

The $\mathcal{N} = 4$ super Yang Mills Lagrangian was first derived by Gliozzi, Scherk and Olive via Kaluza Klein reduction, from a ten-dimensional supersymmetric Lagrangian [35]. A review of various supersymmetric compactification from higher dimensions can be found in [36]. Independent of their discovery, Grimm, Sohnius and Wess [37] constructed the same theory from $\mathcal{N} = 1$ superfields in four spacetime dimensions. The authors all use slightly different notations and

conventions. I will begin from the Lagrangian as it was derived in [35]

$$\begin{aligned}\mathcal{L} = \mathrm{tr}\Big\{ &-\frac{1}{4}\mathfrak{F}_{mp}\mathfrak{F}^{mp} - \sum_{i=1}^{4} i\bar{\psi}_i\bar{\sigma}^m\mathfrak{D}_m\psi_i \\ &+ \frac{g}{2}\sum_{a,i,j}^{6,4,4}\Big(c^{aij}B_a[\psi_j,\psi_i] + \bar{c}^{aij}B_a[\bar{\psi}_j,\bar{\psi}_i]\Big) \\ &- \frac{1}{2}\sum_{a=1}^{6}\mathfrak{D}_m B_a\mathfrak{D}^m B^a + \frac{g^2}{4}\sum_{a,b=1}^{6}[B_a,B_b]^2\Big\}\,.\end{aligned} \tag{4.1.1}$$

The constants c^{aij} and $\bar{c}^{aij}$ are related to the Clifford Dirac matrices of the scalar fields $\mathfrak{so}(6) \simeq \mathfrak{su}(4)$ symmetry. $\mathfrak{D}_m$ is the non-Abelian covariant derivative, defined with the coupling g appearing in the commutator

$$\mathfrak{D}_m(\cdot) = \partial_m(\cdot) + ig[\nu_m,(\cdot)] \tag{4.1.2}$$

and $\mathfrak{F}_{mp}$ is the non-Abelian field strength of the vector boson field ν

$$\mathfrak{F}_{mp} = \partial_m\nu_p - \partial_p\nu_m - ig[\nu_m,\nu_p]\,. \tag{4.1.3}$$

All fields are in adjoint representation and can be expressed in terms of $N \times N$ matrices.

Higgs mechanism

$\mathcal{N} = 4$ super Yang Mills theory is scale invariant. As a consequence, all particles are massless. A realistic hydrogen model, however, contains two fermions with a mass gap of about 2000 units. Masses in $\mathcal{N} = 4$ are given to the fields by applying the Higgs mechanism. To keep the model as simple as possible, only the first scalar field B_1 will acquire a nonzero vacuum expectation value

$$\langle B_1\rangle = v\begin{pmatrix} m_1 & 0 & \cdots & 0 \\ 0 & m_2 & \cdots & 0 \\ \vdots & \vdots & \ddots & \vdots \\ 0 & 0 & \cdots & m_N \end{pmatrix} = b_1 \Rightarrow B_1 = b_1 + \tilde{\mathrm{B}}_1 \tag{4.1.4a}$$

$$\langle B_a\rangle = 0 \quad \forall \quad a \neq 1\,. \tag{4.1.4b}$$

The field $\tilde{\mathrm{B}}_1$ represents the Goldstone bosons, which arise from the symmetry breaking. By giving B_1 a vacuum expectation value, the $\mathfrak{so}(6)$ scalar symmetry is broken to $\mathfrak{so}(5)$. The $U(N)$ representation of B_1 is broken to $\mathrm{U}(N) \to \mathrm{U}(1)^j \times \mathrm{U}(N-j)$ with j being the number of masses for which $m_j \neq 0$.

Mass terms

The Lagrangian in equation 4.1.1 contains a scalar-fermion-fermion interaction term similar to the Yukawa terms in the standard model. Its B_1 interaction then yields the following *fermion* mass term

$$\begin{aligned}\Delta\mathcal{L} &= gc^{aji}\mathrm{tr}\{(B_1)^s_t\psi^t_{iu}\psi^u_{jv} - (B_1)^s_t\psi^t_{ju}\psi^u_{iv}\} \\ &= gc^{1ji}\big[(B_1)^s_s\psi^s_{iu}\psi^u_{js} - (B_1)^s_s\psi^s_{ju}\psi^u_{is}\big] \\ &= gc^{1ji}(m_s - m_u)\psi^s_{iu}\psi^u_{js}\,.\end{aligned} \tag{4.1.5}$$

There are mass terms ($m_{su} = gc^{1ji}(m_s - m_u)$) for all off-diagonal Weyl spinors of each fermionic field. The factor of two disappears by interchanging i and j. Choosing the values of m_s and m_u appropriately, it is possible to construct an electron and proton generation, e.g.

$$m_1 = 0,\ m_2 = 1,\ m_3 = 2000 \qquad v = m_e/g\ . \tag{4.1.6}$$

The Weyl spinors with $U(1)$ charge $(2,1)$ form the electron generation, while spinors charged under $(3,1)$ with m_{31} become the anti-proton generation. Since the proton is oppositely charged to the electron, it is useful to consider particles charged with $(1,3)$ as the proton generation. The choice of indices is arbitrary as long as both pairs share a common $U(1)$ charge, so that they can interact and form bound states.

Note that the diagonal elements of the fermion fields stay massless; they are the gauginos that change fermions into scalars. Also due to the non zero values of c^{1ji} there are exactly four (eight with the $\bar{\psi}$ couplings) mass terms in each generation, giving four massive electrons.

The *vector* mass terms arise from the scalar's kinetic term

$$\begin{aligned}\Delta\mathcal{L} &= -\frac{1}{2}\mathrm{tr}\big\{\mathfrak{D}_m B_a \mathfrak{D}^m B_a\big\} \\ &\Rightarrow \frac{g^2}{2}\mathrm{tr}\big\{[b_1,\nu^m][b_1,\nu_m]\big\} \\ &= g^2\big(m_s m_u + m_u m_s - m_u m_u - m_s m_s\big)\nu_s^{m\ u}\nu_{m\ u}^{s}\end{aligned} \tag{4.1.7}$$

which provides mass terms to the $N^2 - N$ off-diagonal vector bosons while the N diagonal elements stay massless 'photons'.

Scalar mass terms arise from the four point vertex in the scalar potential

$$\Delta\mathcal{L} = \frac{g^2}{2}\mathrm{tr}\{[b_1,B_a]^2\} = g^2\big(m_s m_u + m_u m_s - m_u m_u - m_s m_s\big)B_{a\ s}^{u}B_{a\ u}^{s}\ , \tag{4.1.8}$$

resulting once again in N massless scalars and $N^2 - N$ massive ones. The $N^2 - N$ off-diagonal Goldstone bosons $\tilde{B}_1$ are eaten by the massive vectors while the $N-$diagonal elements becomes massless 'Higgs'. They couple to the mass of the different particles and are the scalar superpartner to the photons.

Summarizing, one finds the mass

$$m \equiv |m_s - m_u| \tag{4.1.9}$$

for every particle of a given generation (s,u).

Gauge fixing

For a complete picture I will briefly mention gauge fixing. Taking a closer

look at the coupling between B_1 and the gauge bosons

$$\begin{aligned}\Delta\mathcal{L} &= -\frac{1}{2}\mathrm{tr}\{\mathfrak{D}_m(b_1+\hat{\mathrm{B}}_1)\mathfrak{D}^m(b_1+\hat{\mathrm{B}}_1)\}\\ &= -\frac{1}{2}\mathrm{tr}\{\partial_m\hat{\mathrm{B}}_1\partial^m\hat{\mathrm{B}}_1 - 2gi[b_1+\hat{\mathrm{B}}_1,\nu^m]\partial_m\hat{\mathrm{B}}_1 - g^2[b_1+\hat{\mathrm{B}}_1,\nu^m]^2\}\\ &= -\frac{1}{2}\mathrm{tr}\{\partial_m\hat{\mathrm{B}}_1\partial^m\hat{\mathrm{B}}_1 - 2gi[b_1,\nu^m]\partial_m\hat{\mathrm{B}}_1 - 2gi[\hat{\mathrm{B}}_1,\nu^m]\partial_m\hat{\mathrm{B}}_1\\ &\quad - g^2[b_1,\nu^m]^2 - g^2[\hat{\mathrm{B}}_1,\nu^m]^2 - 2g^2[b_1,\nu^m][\hat{\mathrm{B}}_1,\nu^m]^2\}\end{aligned}$$

one finds the common terms for propagators, masses of the gauge bosons, interaction vertices, once coupling to g for the vector boson exchange and the other time coupling to the mass as in the usual Higgs mechanism. The second term, however, is not physical, since it couples the Goldstone bosons to the vectors. It contributes to the longitudinal mass component of the gauge bosons and can be canceled by fixing the gauge.

Introducing $G = \partial_m\nu^m + i\xi g[b_1,\hat{\mathrm{B}}_1]$:

$$\begin{aligned}\mathcal{L}_{\mathrm{gf}} &= -\frac{1}{2}\mathrm{tr}\{\xi^{-1}GG\}\\ &= -\frac{1}{2}\mathrm{tr}\{\xi^{-1}\partial_m\nu^m\partial_n\nu^n + 2ig[b_1,\hat{\mathrm{B}}_1]\partial_m\nu^m - \xi g^2[b_1,\hat{\mathrm{B}}_1]^2\} \qquad (4.1.10)\\ &= -\frac{1}{2}\mathrm{tr}\{\xi^{-1}\partial_m\nu^n\partial_n\nu^m + 2ig[b_1,\nu^m]\partial_m\hat{\mathrm{B}}_1 - \xi g^2[b_1,\hat{\mathrm{B}}_1]^2\}\ .\end{aligned}$$

Here, I partially integrated in the last line so that the second term takes the same form as in the previous calculation. They have opposite signs and cancel with each other.

(anti-)BPS multiplets

The Higgs mechanism breaks the $\mathfrak{so}(6) \simeq \mathfrak{su}(4)$ scalar symmetry to $\mathfrak{so}(5) \simeq \mathfrak{usp}(4)$. Each particle generation is described by a (anti-)BPS multiplet. Recalling from chapter 3, the creation and annihilation operators are

$$\{a^I_{a\pm}, (a^J_{b\pm})^\dagger\} = -(2m \pm z)\delta^I_J\delta^b_a\ . \qquad (4.1.11)$$

Here the indices a, b correspond to the little group $\mathfrak{so}(3)$, and the indices I, J to the R-symmetry $\mathfrak{usp}(4)$. The rest symmetry is then described by $\mathfrak{so}(3)\otimes\mathfrak{usp}(4)$. The corresponding particle spectrum has been analyzed in the past, e.g. in [38] [39]

$$\Phi_{(\text{anti-})\mathrm{BPS}} = (\mathbf{1},\mathbf{5})_\phi \oplus (\mathbf{2},\mathbf{4})_\psi \oplus (\mathbf{3},\mathbf{1})_\nu\ . \qquad (4.1.12)$$

The first index stands for the representation of the little group $\mathfrak{so}(3)$, while the second one is for the representation of the R-symmetry $\mathfrak{so}(5)$. It confirms the explicit results found in the previous analysis with five massive scalars, four massive fermions and one massive vector boson.

4.2 Energy spectrum

The previously constructed model allows a total of 256 possible bound states. There are

$$\begin{aligned}
&(\psi_{\mathrm{e}} \otimes \psi_{\mathrm{p}}) = (4_{\mathrm{particles}} \cdot 2_{\mathrm{Spin}}) \cdot (4_{\mathrm{particles}} \cdot 2_{\mathrm{Spin}}) = 64 \\
&(\nu_{\mathrm{e}} \otimes \nu_{\mathrm{p}}) = (1_{\mathrm{particles}} \cdot 3_{\mathrm{Spin}}) \cdot (1_{\mathrm{particles}} \cdot 3_{\mathrm{Spin}}) = 9 \\
&(\nu_{\mathrm{e}} \otimes \phi_{\mathrm{p}}) = (1_{\mathrm{particles}} \cdot 3_{\mathrm{Spin}}) \cdot (5_{\mathrm{particles}} \cdot 1_{\mathrm{Spin}}) = 15 \\
&(\phi_{\mathrm{e}} \otimes \nu_{\mathrm{p}}) = (5_{\mathrm{particles}} \cdot 1_{\mathrm{Spin}}) \cdot (1_{\mathrm{particles}} \cdot 3_{\mathrm{Spin}}) = 15 \\
&(\phi_{\mathrm{e}} \otimes \phi_{\mathrm{p}}) = (5_{\mathrm{particles}} \cdot 1_{\mathrm{Spin}}) \cdot (5_{\mathrm{particles}} \cdot 1_{\mathrm{Spin}}) = 25 \\
&\rightarrow 128 \text{ bosonic bound states}
\end{aligned} \tag{4.2.1}$$

and similarly

$$\begin{aligned}
&(\psi_{\mathrm{e}} \otimes \nu_{\mathrm{p}}) = (4_{\mathrm{particles}} \cdot 2_{\mathrm{Spin}}) \cdot (1_{\mathrm{particles}} \cdot 3_{\mathrm{Spin}}) = 24 \\
&(\nu_{\mathrm{e}} \otimes \psi_{\mathrm{p}}) = (1_{\mathrm{particles}} \cdot 3_{\mathrm{Spin}}) \cdot (4_{\mathrm{particles}} \cdot 2_{\mathrm{Spin}}) = 24 \\
&(\psi_{\mathrm{e}} \otimes \phi_{\mathrm{p}}) = (4_{\mathrm{particles}} \cdot 2_{\mathrm{Spin}}) \cdot (5_{\mathrm{particles}} \cdot 1_{\mathrm{Spin}}) = 40 \\
&(\phi_{\mathrm{e}} \otimes \psi_{\mathrm{p}}) = (5_{\mathrm{particles}} \cdot 1_{\mathrm{Spin}}) \cdot (4_{\mathrm{particles}} \cdot 2_{\mathrm{Spin}}) = 40 \\
&\rightarrow 128 \text{ fermionic bound states.}
\end{aligned} \tag{4.2.2}$$

In analogy to the previous chapter, it is useful to get a better understanding of the spectrum by analyzing it in terms of its symmetries. As in the $\mathcal{N}=2$ case, the two supermultiplets bind together in leading order by exchange of photon and massless 'Higgs'. The Coulomb attraction is twice as strong, but possibly broken by relativistic effects. The spectrum then transforms as

$$\mathcal{S} = \Phi_{\mathrm{e}}^{\mathrm{BPS}} \otimes \Phi_{\mathrm{p}}^{\text{Anti-BPS}} = \Phi_{\mathrm{BS}}^{\text{non BPS}} \tag{4.2.3}$$

a single multiplet built from the Clifford vacuum Ω_0. Here, $2z_{\mathrm{e}} = |m_1 - m_2|$ and $2z_{\mathrm{p}} = |m_3 - m_1|$ such that $2m_{\mathrm{BS}} > z_{\mathrm{e}} + z_{\mathrm{p}}$. A quick check reveals that the long non-BPS $\mathcal{N} = 4$ multiplet

$$\begin{cases}
1 & \times & \lambda = \pm 2 \\
8 & \times & \lambda = \pm \frac{3}{2} \\
28 & \times & \lambda = \pm 1 \\
56 & \times & \lambda = \pm \frac{1}{2} \\
70 & \times & \lambda = 0
\end{cases} \tag{4.2.4}$$

matches the 128 bosonic and fermionic bound states from 4.2.1 and 4.2.2. From appendix A.3 it is known that the long multiplet transforms trivially under $\mathfrak{so}(3)$ excitations

$$V_l \otimes (\Phi_{\mathrm{e}}^{\mathrm{BPS}} \otimes \Phi_{\mathrm{p}}^{\text{Anti-BPS}}) = \Phi_l^{\mathrm{BS}} \,. \tag{4.2.5}$$

Since $\Phi^{\text{non BPS}}$ is determined from the product of BPS and anti-BPS multiplets, it transforms with 4.1.12 as

$$\begin{aligned}
&\Phi_{\mathrm{e}}^{\mathrm{BPS}} \otimes \Phi_{\mathrm{p}}^{\text{anti-BPS}} \\
&= \big((\mathbf{1},\mathbf{5})_\phi \oplus (\mathbf{2},\mathbf{4})_\psi \oplus (\mathbf{3},\mathbf{1})_\nu\big)_{\mathrm{e}} \otimes \big((\mathbf{1},\mathbf{5})_\phi \oplus (\mathbf{2},\bar{\mathbf{4}})_{\bar{\psi}} \oplus (\mathbf{3},\mathbf{1})_\nu\big)_{\mathrm{p}} = \mathbf{256}
\end{aligned} \tag{4.2.6}$$

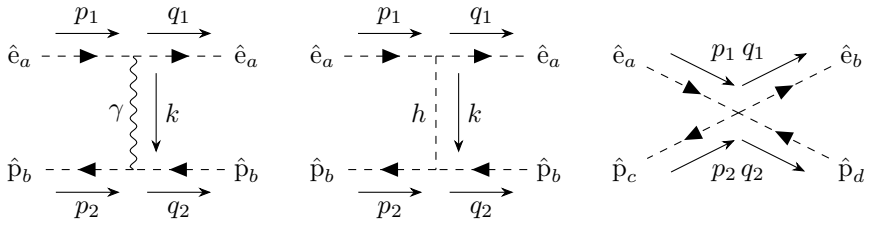

Figure 4.1: The three tree level Feynman diagrams of $\hat{\mathrm{e}}\ \hat{\mathrm{p}} \to \hat{\mathrm{e}}\ \hat{\mathrm{p}}$ scattering. $\hat{\mathrm{e}}$ and $\hat{\mathrm{p}}$ denote to the scalar superpartners or electron and proton.

under $\mathfrak{so}(5)$. The **256** can be decomposed into irreducible representation according to

$$\begin{cases} \nu_m\ \mathbf{1} & \to \begin{cases} (\nu_\mathrm{e}, \nu_\mathrm{p}) & \mathbf{1} \otimes \mathbf{1} = \mathbf{1} \\ (\nu_\mathrm{e}, \bar{\psi}_\mathrm{p}) & \mathbf{1} \otimes \bar{\mathbf{4}} = \bar{\mathbf{4}} \\ (\nu_\mathrm{e}, B_\mathrm{p}) & \mathbf{1} \otimes \mathbf{5} = \mathbf{5} \end{cases} \\ \psi_i\ \mathbf{4} & \to \begin{cases} (\psi_\mathrm{e}, \nu_\mathrm{p}) & \mathbf{4} \otimes \mathbf{1} = \mathbf{4} \\ (\psi_\mathrm{e}, \bar{\psi}_\mathrm{p}) & \mathbf{4} \otimes \bar{\mathbf{4}} = \mathbf{16} = \mathbf{1} \oplus \mathbf{5} \oplus \mathbf{10} \\ (\psi_\mathrm{e}, B_\mathrm{p}) & \mathbf{4} \otimes \mathbf{5} = \mathbf{20} = \mathbf{4} \oplus \mathbf{16} \end{cases} \\ B_a\ \mathbf{5} & \to \begin{cases} (B_\mathrm{e}, \nu_\mathrm{p}) & \mathbf{5} \otimes \mathbf{1} = \mathbf{5} \\ (B_\mathrm{e}, \bar{\psi}_\mathrm{p}) & \mathbf{5} \otimes \bar{\mathbf{4}} = \mathbf{20} = \bar{\mathbf{4}} \oplus \mathbf{16} \\ (B_\mathrm{e}, B_\mathrm{p}) & \mathbf{5} \otimes \mathbf{5} = \mathbf{25} = \mathbf{1} \oplus \mathbf{10} \oplus \mathbf{14} \end{cases} \\ \bar{\psi}_i\ \bar{\mathbf{4}} & \to \cdots \\ \quad \vdots \end{cases} . \tag{4.2.7}$$

Here, the **25** representation of the scalar-scalar bound state decomposes into the trace **1**, the antisymmetric **10** and the traceless symmetric **14** representation. Since the **14** only appears in the scalar-scalar bound states, its eigenvalue gets no contributions from mixing with other bound states. The energy eigenvalue of the long multiplet can then be determined solely from the **14** representation, as all representations have to share the same energy.

4.3 Energy splitting

There are three tree level diagrams presented in figure 4.1 for the scattering process $\hat{\mathrm{e}}\ \hat{\mathrm{p}} \to \hat{\mathrm{e}}\ \hat{\mathrm{p}}$. The two particle families interact via exchange of a (1,1) photon and higgs. Additionally, there is a contribution coming from the 4-point scalar vertex. The **first** amplitude describing the exchange of a photon is

$$\begin{aligned} i\mathcal{M}_1 \simeq \frac{4 m_\mathrm{e} m_\mathrm{p} g^2}{(\vec{p} - \vec{q})^2} \Bigg[1 + (\vec{p}^2 + \vec{q}^2) \left(\frac{1}{4 m_\mathrm{e}^2} + \frac{1}{4 m_\mathrm{p}^2} \right) - \frac{1}{4 m_\mathrm{e} m_\mathrm{p}} \\ \left((1 - \xi) \frac{(\vec{p}^2 - \vec{q}^2)^2}{(\vec{p} - \vec{q})^2} - (\vec{p} + \vec{q})^2 \right) \Bigg] . \end{aligned} \tag{4.3.1}$$

The **second** amplitude coming from a massless scalar exchange is simply

$$i\mathcal{M}_2 = 4m_e m_p g^2 \left[\frac{1}{k^2}\right] . \tag{4.3.2}$$

The first two amplitudes correspond to an overall shift to any scalar-scalar bound state, while the **third** one

$$i\mathcal{M}_3 \propto \pm g^2 , \tag{4.3.3}$$

has a magnitude, which depends on the involved particles. From the following table

	aa	ab	ba	bb
aa	0	0	0	$2g^2$
ab	0	$-g^2$	$-g^2$	0
ba	0	$-g^2$	$-g^2$	0
bb	$2g^2$	0	0	0

one can determine its contribution to a given bound state. Since only $\mathcal{M}_3$ is responsible for mixing within the scalar-scalar bound state, it solely determines the **14**-eigenvalue, which is $i\mathcal{M}_{14} = -2g^2$. The normalized amplitude of $\mathcal{M} = \mathcal{M}_1 + \mathcal{M}_2 + \mathcal{M}_{14}$ then becomes

$$\begin{aligned}\mathcal{M}_{\text{NR}} = \frac{g^2}{(\vec{p}-\vec{q})^2}\Bigg[2 + \frac{1}{m_e m_p}\left(\vec{p}^2 + \frac{(\vec{p}-\vec{q})^2}{4} - \frac{(\vec{p}\cdot(\vec{p}-\vec{q}))^2}{(\vec{p}-\vec{q})^2}\right) - \frac{(\vec{p}-\vec{q})^2}{4m_e m_p} \\ - \frac{\vec{p}^2+\vec{q}^2}{4}\left(\frac{1}{m_e^2}+\frac{1}{m_p^2}\right) - \frac{(\vec{p}-\vec{q})^2}{2m_e m_p}\Bigg] ,\end{aligned} \tag{4.3.4}$$

which results in the energy potential

$$\begin{aligned}V(\vec{r},\vec{p}) = \alpha\Bigg[-\frac{1}{m_e m_p}\left(\frac{\vec{p}^2}{2r} + \frac{(\vec{r}\cdot\vec{p})^2}{2r^3} + \pi\delta^3(\vec{r})\right) + \frac{\vec{p}^2}{r}\left(\frac{1}{4m_e^2}+\frac{1}{4m_p^2}\right) \\ + \frac{3\pi\delta^3(\vec{r})}{m_e m_p}\Bigg] - \frac{\vec{p}^4}{8}\left(\frac{1}{m_e^3}+\frac{1}{m_p^3}\right) ,\end{aligned} \tag{4.3.5}$$

where momentum conservation was used $\vec{p}^2 + \vec{q}^2 \sim 2\vec{p}^2$. The energy corrections are then once again determined with first order perturbation theory. Here, one has to be careful, since the Coulomb potential is twice as strong, all αs coming from the EV carry an additional factor of two with them. The results for $l \neq 0$ are then:

$$\delta E_{n,l}(\alpha^4) = \frac{\alpha^4\mu}{n^4}\left[\frac{\mu^2}{m_e m_p}\left(\frac{8n}{2l+1} - 6\right) - \left(\frac{8n}{2l+1} + 4\right)\right] . \tag{4.3.6}$$

And the results for $l = 0$ are:

$$\begin{aligned}\delta E_{n,0}(\alpha^4) &= \delta E_{n,l=0}(\alpha^4) + \frac{\mu\alpha^4}{n^3}\left[\frac{24\mu^2}{m_e m_p}\right] \\ &= \frac{\alpha^4\mu}{n^4}\left[\frac{\mu^2}{m_e m_p}\left(8n+18\right) - \left(8n+4\right)\right] .\end{aligned} \tag{4.3.7}$$

It is obvious due to the explicit l-dependence that the $\mathfrak{so}(4)$ symmetry is broken.

Chapter 5

Discussion

The results from the previous chapter are in a strong contradiction with the observation made by Caron-Huot and Henn [3], who found the n^2 degeneracy to be preserved for relativistic corrections. In this chapter, I will attempt to give a complete discussion why this contradiction exists. For this, I begin with considering the even simpler model of a massive charged scalar coupled to a static potential via a photon and a massless scalar. This is a simplified version of my previous model, and also of hydrogen in $\mathcal{N} = 2$ with a heavy proton in the $m_{\rm p} \to \infty$ mass limit. The system is evaluated by means of the Klein-Gordon equation and comparison to the time independent Schroedinger equation. It turns out that there is a discrepancy between the field theoretical approach and relativistic quantum mechanics.

Furthermore, I will comment on other issues which have been treated inconsistently or neglected before, such as the choice of Coulomb gauge and other cross particle scattering diagrams, the missing $\mathcal{O}(\alpha^3)$ corrections, and finally interactions with other particles and massive intermediate particle states.

Alongside this I will give a discussion about future studies and directions.

5.1 Relativistic quantum mechanics

Consider a system of two charged scalars, both coupling to a massless vector (photon) and a massless scalar ('Higgs'). In the heavy proton limit, it is equivalent to a scalar (selectron) with mass m coupling to a static force field. The system satisfies the slightly modified Klein-Gordon equation

$$\Big[-(\partial_t - iV_\gamma)^2 + \Box - (m - V_\varphi)^2 \Big] \phi = 0 \tag{5.1.1}$$

where m denotes, from now on, the electron mass. The potentials are given by

$$V_\gamma = V_\varphi = \frac{\alpha}{r} \qquad -\partial_t = iE_t \ . \tag{5.1.2}$$

This is in accordance with the leading order contributions from the field theoretical approach of photon and scalar exchange. The 4-point vertex has no impact, since the proton mass is taken to be $m_p \to \infty$. Then equation 5.1.1

becomes

$$\left[(E+m)(E-m+\frac{2\alpha}{r})+\Box\right]\phi=0\ . \tag{5.1.3}$$

The energy is easily found by comparing this to the solution of the time independent Schroedinger equation, which can be derived via separation of variables

$$\begin{aligned}&\left[-\frac{\Box}{2\mu}-\frac{\alpha}{r}\right]\psi=\epsilon\psi \quad \to \epsilon=-\frac{\mu\alpha^2}{2n^2}\\ \Leftrightarrow&\left[-\frac{1}{2\mu}\left(-(\partial_r)^2-\frac{2}{r}\partial_r+\frac{l(l+1)}{r^2}\right)-\frac{\alpha}{r}\right]\psi=\epsilon\psi\ .\end{aligned} \tag{5.1.4}$$

One finds

$$\begin{aligned}E-m&=-\left(\frac{E+m}{2}\right)\frac{(2\alpha)^2}{2n^2}\\ \Leftrightarrow E&=m\left(1-\frac{2\alpha^2}{n^2+\alpha^2}\right)=m\left[1-\frac{2\alpha^2}{n^2}+\frac{2\alpha^4}{n^4}+\mathcal{O}(\alpha^6)\right]\ .\end{aligned} \tag{5.1.5}$$

In contradiction to the field theoretical calculations, this result is independent of l and preserves the $\mathfrak{so}(4)$ symmetry, confirming [3].

It is known that the relativistic QM approach yields the same result as the field theoretical setup in the heavy proton limit where the proton is approximated as a static Coulomb source [24]. The Klein-Gordon equation for such a model is given by

$$\left[\left(E+\frac{\alpha}{r}\right)^2+\Box-m^2\right]\phi=0 \tag{5.1.6}$$

and can be compared to the time independent Schroedinger equation in 5.1.4. The solution is found in many books about relativistic quantum mechanics such as [40]. The bound state energy is then

$$\begin{aligned}\frac{E^2-m^2}{2E}&=-\frac{1}{2}\frac{\alpha^2 E}{x^2} \qquad\qquad x=n-\frac{\alpha^2}{2l+1}+\mathcal{O}(\alpha^4)\\ \Leftrightarrow E&=m\left[1+\frac{\alpha^2}{x^2}\right]^{-\frac{1}{2}}=m\left[1-\frac{\alpha^2}{2n^2}-\frac{\alpha^4}{2n^4}\left(\frac{n}{l+1/2}-\frac{3}{4}\right)+\mathcal{O}(\alpha^6)\right]\end{aligned} \tag{5.1.7}$$

which is equivalent to the result of the field theoretical approach coming from the scattering amplitude 4.3.1, and coincides with the fine structure splitting of atomic hydrogen in equation 2.2.14 by replacing $j \to l$ due to the lack of spin-orbit interaction in a scalar-scalar bound state.

Hence, the problem must come from the massless scalar exchange. The field theoretical approach only using the 'Higgs' exchange yields a $E(\alpha^4)$ energy coming from the relativistic 2.2.11 and the normalization correction 2.2.8

$$\begin{aligned}\delta E(\alpha^4)&=-\frac{1}{8m^3}\langle\phi|\,\vec{p}^4\,|\phi\rangle+\frac{1}{4m^2}\langle\phi|\,\frac{\vec{p}^2}{r}\,|\phi\rangle\\ &=-\frac{(m\alpha)^4}{8n^4m^3}\left[\frac{4n}{l+1/2}-3\right]+\left(\frac{\alpha}{m^2}\right)\frac{(m\alpha)^3}{4n^4}\left[\frac{2n}{l+1/2}-1\right]=\frac{m\alpha^4}{8n^4}\ .\end{aligned} \tag{5.1.8}$$

The Klein-Gordon equation for a massless scalar exchange coupling to the mass is

$$\left[E^2 + \Box - \left(m - \frac{\alpha}{r}\right)^2\right]\phi = 0\,. \tag{5.1.9}$$

Comparison with equation 5.1.4 yields for the energy

$$\begin{aligned}\frac{E^2 - m^2}{2m} &= -\frac{1}{2}\frac{\alpha^2 m}{x^2} \qquad\qquad x = n + \frac{\alpha^2}{2l+1} + \mathcal{O}(\alpha^4) \\ \Leftrightarrow E &= m\left[1 - \frac{\alpha^2}{x^2}\right]^{\frac{1}{2}} = m\left[1 - \frac{\alpha^2}{2n^2} - \frac{\alpha^4}{8n^4} + \frac{\alpha^4}{(2l+1)n^3} + \mathcal{O}(\alpha^6)\right].\end{aligned} \tag{5.1.10}$$

The energy corrections at α^4 in equations 5.1.8 and 5.1.10 differ. One immediately sees that the difference arises from a 'missing' factor of two in front of the second operator in 5.1.8, coming from the normalization in the field theoretical approach.

This can be shown by comparing the operators in both approaches. The energy in terms of operators can be naively sketched (ignoring normal ordering) as

$$\begin{aligned}E &\sim \sqrt{m^2 + \vec{p}^2 - 2mV + V^2} \sim m\left[1 + \frac{\vec{p}^2 - 2mV + V^2}{m^2}\right]^{\frac{1}{2}} \\ &\sim m + \frac{\vec{p}^2}{2m} - V + \frac{\cancel{V^2}}{\cancel{2m}} - \frac{\vec{p}^4}{8m^3} + \frac{\vec{p}^2 V}{2m^2} - \frac{\cancel{V^2}}{\cancel{2m}} + \mathcal{O}(\alpha^5) \\ &\sim -\frac{m\alpha^4}{8n^4} + \frac{m\alpha^4}{(2l+1)n^3}\end{aligned} \tag{5.1.11}$$

reproducing the energy obtained earlier. While in the field theoretical approach, one finds the operators

$$H - m_{\mathrm{p}} \sim m + \frac{\vec{p}^2}{2m} - V - \frac{\vec{p}^4}{8m^3} + \frac{\vec{p}^2 V}{4m^2} + \mathcal{O}(\alpha^5) \sim \frac{m\alpha^4}{8n^4}\,. \tag{5.1.12}$$

Here the difference of the previously mentioned factor of 2 becomes even more clear.

The operator approach for the model with 'Higgs' and photon exchange described by the Klein-Gordon equation in 5.1.1 yields

$$\begin{aligned}E &\sim -V \pm \left[V^2 + \vec{p}^2 + m^2 - 2mV\right]^{\frac{1}{2}} \\ &\sim m - 2V + \frac{\vec{p}^2}{2m} + \frac{\cancel{V^2}}{\cancel{2m}} - \frac{\vec{p}^4}{8m^3} + \frac{\vec{p}^2 V}{2m^2} - \frac{\cancel{V^2}}{\cancel{2m}} + \mathcal{O}(\alpha^5) \\ &\sim \frac{2\alpha^4}{n^4}\,.\end{aligned} \tag{5.1.13}$$

In the last line one has to be careful when taking the EV that one replaces $\alpha_0 \to 2\alpha$, since the Coulomb attraction is twice as strong. As a consequence, the l-dependence from equation 5.1.11 drops out. The energy correction at $\mathcal{O}(\alpha^4)$ in

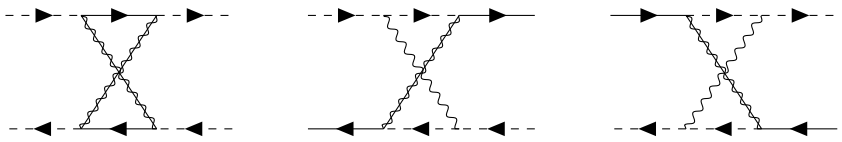

Figure 5.1: One loop cross scattering diagrams describing the exchange of gaugino and photon. There are many more possible diagrams involving different combinations of on shell scalars and fermions.

equation 5.1.5 is reproduced, showing that this procedure is consistent. Again, the difference between quantum mechanical and the field theoretical approaches lies in the factor of two in front of the operator $\frac{\vec{p}^2}{r}$. Summarizing, there appears to be an inconsistency in the field theoretical approach. This might be resolved by considering one loop diagrams, as discussed in the next section.

5.2 Cross particle scattering

Derivation of all relevant operator terms with energy corrections of $\mathcal{O}(\alpha^4)$ was based on the usage of Coulomb gauge in the case of QED. As mentioned in chapter 2, it has been shown by Lindgren in 1990 [21] that only in this particular choice of gauge the leading contributions, coming from cross photon scattering diagrams, such as shown in figure 2.2 cancel. The gauge dependent term in equation 2.2.7 or 4.3.1 contributes at energy $\delta E_{\text{cross}} \propto \alpha^4$. This can also naively be seen from the cross scattering diagram. Each photon contributes in leading order with the Coulomb potential $\frac{1}{r} \sim \alpha$ and there are four involved vertices, giving in total another α^2.

The study of SQED bound states without an exchanged scalar as in [1] [2] then also made use of the choice $\xi = 0$. However, the question remains why several additional 'supersymmetric' cross scattering diagrams involving gauginos and photons, such as shown in figure 5.1 should not contribute at $\mathcal{O}(\alpha^4)$. One could argue again that the leading operator coming from a single gaugino exchange contributes with α^2 and therefore these new diagrams should contribute at least $\mathcal{O}(\alpha^5)$. Further studies in the future are needed to indeed show that cross gaugino scattering diagrams do not contribute at $\mathcal{O}(\alpha^4)$. The latter two diagrams in figure 5.1 do not contribute to the **14** scalar-scalar bound state representation of the $\mathcal{N}=4$ model.

In contrast to the cross gaugino scattering, cross scalar and mixed cross scalar and photon scattering will certainly contribute to the energy spectrum at $\mathcal{O}(\alpha^4)$. The diagrams presented in figure 5.2 are therefore relevant not only for the $\mathcal{N}=4$ model, but also for the $\mathcal{N}=2$ case. This can be argued as I have done for the Coulomb gauge and cross photons. It becomes even more clear when comparing scalar and photon propagators. They both give the same leading order contribution $\sim \frac{\mu}{r}$. For a photon in Feynman gauge with $\xi = 1$, the gauge dependent term in equation 2.2.7 or 4.3.1, which contributes at $\mathcal{O}(\alpha^4)$ disappears, meaning that the cross scattering diagrams certainly contribute. For future studies it would be interesting if there is a choice of gauge, such as Coulomb for QED, where all relevant terms contributing at $\mathcal{O}(\alpha^4)$ can be solely determined from tree level diagrams, in a theory involving a photon with

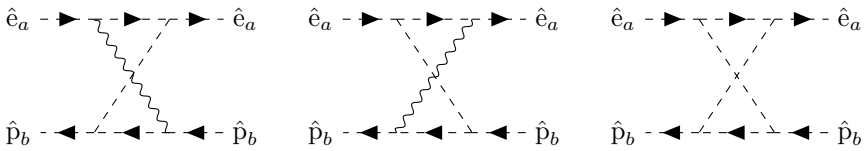

Figure 5.2: Additional one loop diagrams which can contribute to the bound state energy at α^4.

a scalar superpartner.

5.3 Radiative corrections

It is known that radiative gaugino and photon correction for supersymmetric hydrogen contribute at $\mathcal{O}(\alpha^5)$ [2] and are therefore of no relevance for this thesis. In [3], however, several energy corrections of $\mathcal{O}(\alpha^3)$ have been found, see equation 4.0.1. They are attributed to a Lamb shift coming from ultrasoft scalar exchanges. Those are supposed to appear earlier by two orders in α, since they are, in contrast to the photon, not dipole suppressed. Radiative corrections in QED are best investigated with dimensional regularization, a most symmetry preserving method, introduced by 't Hooft and Veltman [41].

The main contribution of the Lamb shift, except for the vacuum polarization, is the correction to the electron vertex. The scalar-scalar-Higgs electron vertex contributes to a Feynman diagram with

$$V_{ssh} = 2mg\big(\mathbf{1} + \delta V_i + \mathcal{O}(\alpha^2)\big) \tag{5.3.1}$$

where δV_i is a correction of order α. Figure 5.3 shows the usual radiative three vertex correction. It is determined by integrating over the loop momentum k

$$\delta V_i = (2mg)^2 \int \frac{\mathrm{d}^4 k}{(2\pi)^4} \frac{1}{k^2 - m^2} \frac{1}{(k+q)^2 - m^2} \frac{1}{(k-p)^2} \,. \tag{5.3.2}$$

The integral is solved by introducing Feynman parameters and Wick rotating the time coordinate by 90 degrees counterclockwise in the complex plane to obtain an Euclidean 4-momentum. It can then be analyzed with dimensional regularization, which has been partly carried out in [42]. The solution suffers from infrared (IR) and ultraviolet (UV) divergences. While the UV divergences should cancel as a consequence from supersymmetry, and it should be IR protected by the mass, a full treatment of all divergences goes beyond the scope of this thesis.

It is important to point out that, in order to get $\mathcal{O}(\alpha^3)$ energy corrections, one needs to find finite terms for δV_1 independent of the momentum operator. This guarantees that they are essentially a correction to the Coulomb potential, which are l independent and therefore automatically preserve the $\mathfrak{so}(4)$-symmetry. Moreover, these vertex corrections imply additional l independent contributions at $\mathcal{O}(\alpha^4)$ coming e.g. from additional corrections to the proton vertex, which further highlights the incompleteness of the finite mass $\mathcal{O}(\alpha^4)$ calculation in chapter 4.

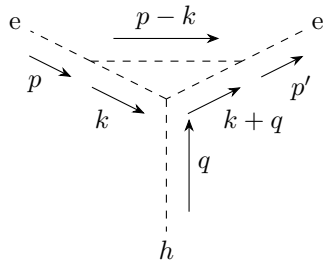

Figure 5.3: Radiative correction to the three scalar-scalar-Higgs vertex due to a Higgs exchange between the two selectrons.

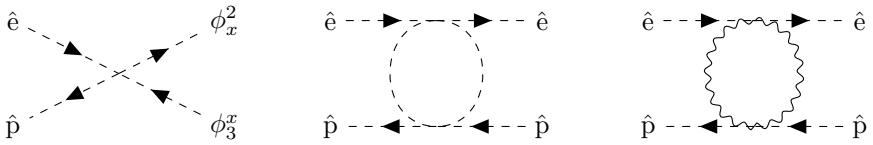

Figure 5.4: (i) Decay of the scalar-scalar bound state into two other scalars. (ii) + (iii) Additional one loop diagrams involving two four point vertices and two virtual bosonic particles.

5.4 Decay

The hydrogenlike bound state in $\mathcal{N}=4$ can decay over the four point scalar vertex

$$B^2_{1\,a}B^1_{3\,a}B^3_{x\,b}B^x_{2\,b} \tag{5.4.1}$$

into various possible other particles as shown in the first diagram of figure 5.4

The majority of these decays are suppressed by adjusting the masses in section 4.1, such that the two outgoing particles with $U(1)$ charges (2,x) and (x,3) are very heavy. Due to energy conversation, the two outgoing particles have to be lighter than the bound state. Hence, all m_is from section 4.1 have to be non-zero. Their values are chosen to be $m_j >> m_3, \forall j > 3$, so interactions with particles of other generations can safely be neglected in the non relativistic limit. The $U(N)$ representation of B_1 is therefore broken to $U(1)^N$.

There is one interesting decay left; when the decay involves a massless scalar (ϕ) of charge (1,1), (2,2) or (3,3) the other decay particle (2,3) or (3,2), from now on called χ, has a smaller mass $m_\chi = m_\mathrm{p} - m_\mathrm{e} < m_\mathrm{p} + m_\mathrm{e} = m_\mathrm{bound}$ than the bound state. Hence, there is a significant possibility for the ground state to decay. The decay width is then proportional to [20]

$$\Gamma(\hat{\mathrm{e}}\ \hat{\mathrm{p}} \to \chi\phi) \propto |\mathcal{M}|^2|\psi(0)|^2 \sim \alpha^5\ . \tag{5.4.2}$$

In section 5.2, contributions from loop diagrams involving the exchange of two bosons have been discussed. This can also happen over two four vertices as presented in (ii) and (iii) of figure 5.4. These two diagrams, which allow the exchange of any kind of boson, are in fact a correction to the four point vertex. Hence, they contribute at energies of $\mathcal{O}(\alpha^5)$.

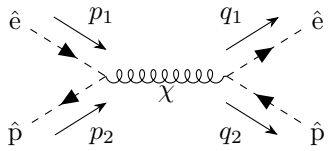

Figure 5.5: Electron and proton decay into a χ which then decays again into an electron and proton. This diagram can give contributions of $\mathcal{O}(\alpha^4)$.

There is also another allowed three vertex decay into the massive vector boson

$$\hat{\mathrm{e}}\ \hat{\mathrm{p}} \to \tilde{\chi} \to \hat{\mathrm{e}}\ \hat{\mathrm{p}}\ . \tag{5.4.3}$$

A comparison to positronium shows that the annihilation of electron and positron to a photon and the subsequent decay into electron and positron does give a bound state energy contribution at $\mathcal{O}(\alpha^4)$. This suggests that the diagram shown in figure 5.5 also gives contributions at the same order. However, there is one major difference to the positronium case $\tilde{\chi}$ is a massive vector. It therefore seems more reasonable to compare its contribution to the exchange of a Z boson in atomic muonium. Here, it was found that it indeed contributes at $\mathcal{O}(\alpha^4)$, but is once again heavily suppressed by the mass [43]. This also holds for the intermediate state of a $\tilde{\chi}$ particle. Furthermore, the on-shell χ belongs to a massive BPS multiplet, hence, this diagram will not contribute to the **14** representation of the non BPS bound state.

Chapter 6

Outlook

The analysis in the previous chapters of the different energy spectra has shown that splitting with more supersymmetry is milder and simplified. In real world hydrogen, the spectrum shows a dependence on the angular momentum l and spin S of the involved fermions; in SQED it only depends on the superspin j of a given multiplet. My analysis showed that for $\mathcal{N}=2$ and $\mathcal{N}=4$ the spectrum contains only a single massive non-BPS multiplet for any given excitation. In the heavy proton limit, I found when using relativistic quantum mechanics that even the $\mathfrak{so}(4)$ Coulomb symmetry is preserved for energy corrections at $\mathcal{O}(\alpha^4)$.

On the other hand, the discussion in the previous chapter showed the limits of the field theoretical approach used for the majority of this thesis. A full treatment of relativistic corrections at $\mathcal{O}(\alpha^4)$ is a tedious exercise and involves the calculation of several different loop diagrams, such as the cross scattering of force carriers and radiative corrections. It would be interesting to find another simpler approach to tackle bound state problems involving a massless scalar as a superpartner of the photon, which can also reproduce the $\mathcal{O}(\alpha^3)$ corrections found in [3].

In the case of bound state problems in QED, there are effective field theories that greatly simplify the calculations. One popular theory is (p)NRQED. Non-Relativistic QED (NRQED) was proposed by Caswell and Lepage in 1986 [44]. It is based on the fact that there are three different energy scales in non relativistic problems: the masses of the involved particles (also called hard scale $\sim m$), the particle momentum (soft scale) $\sim m\alpha$ and the utrasoft scale describing kinetic and bound state energy $\sim m\alpha^2$.

As a consequence of that, usual Feynman diagrams contribute at many different orders in the coupling constant α. NRQED integrates out the hard scale $\sim m$ and, after matching the one loop results between QED and NRQED, it is a straightforward task to reproduce the usual Lamb shift by introducing a cut off and photon mass [45].

pNRQED is then an extension of NRQED. Here, in addition to the hard scale, the soft scale is also integrated out. It is therefore of particular interest for the $\mathfrak{so}(4)$ bound state problem, where the $\mathcal{O}(\alpha^3)$ corrections found by Caron-Huot and Henn were attributed to ultrasoft scalars. Using the techniques of dimensional regularisation pNRQED was used to calculate Lamb shift corrections [46].

For future studies we intend to use the pNRQED framework, and extend it

to incorporate the contribution of an additional massless scalar field. At the same time, the Hamiltonian can be heavily simplified by only considering a scalar-scalar bound state, dropping all spin dependent operators. This would then be similar to the calculations of a static potential in $\mathcal{N}=4$ super Yang Mills, which have been carried out in 2007 by Pineda [47].

Acknowledgements

I want to thank my supervisor Professor Yuji Tachikawa for many interesting and productive discussions and giving me this great opportunity to research one year at Kavli IPMU. Next, I am grateful to Professor Guido Festuccia for accepting me as a master student and providing me with valuable feedback from the other side of the world. I am happy to have enjoyed many interesting discussions about physics over the past months with Itamar Yaakov. I would also like to thank Benjamin Thorne and Xiangchong Li for the great company during lunch, tea time or the many hours spend in the office. The collaboration with Sakata Yusuke and Takemasa Yamaura is greatly acknowledged. Furthermore, I want to thank Thomas Dawson for proofreading and helping me with the language. Finally, I want to thank my family for all the support no matter where I go.

Appendix A

Appendix

A.1 Conventions and identities

Conventions

I use the metric $\eta^{nm} = \text{diag}(-1, 1, 1, 1)$. The gamma matrices are defined by

$$\gamma^m = \begin{pmatrix} 0 & \sigma^m \\ \bar{\sigma}^m & 0 \end{pmatrix} \qquad \gamma^5 = \begin{pmatrix} -i & 0 \\ 0 & i \end{pmatrix} \tag{A.1.1}$$

where $\sigma = (-\mathbf{1}, \vec{\sigma})$, $\bar{\sigma} = (-\mathbf{1}, -\vec{\sigma})$. The epsilon tensor used in this thesis is $\epsilon^{\alpha\beta} = \begin{pmatrix} 0 & 1 \\ -1 & 0 \end{pmatrix} = -\epsilon_{\alpha\beta}$, which is needed to raise and lower spinor indices $\psi^\alpha = \epsilon^{\alpha\beta}\psi_\beta$. Anti-spinors are defined according to $\bar{u}(k) = u^\dagger(k)\gamma^0$.

Superfields

The particle representation of a $\mathcal{N} = 1$ chiral field is

$$\Phi = \phi + \sqrt{2}\theta\psi + \theta\theta F \; . \tag{A.1.2}$$

A vector field in Wess-Zumino gauge contains the particles

$$V = -\theta\sigma^m\bar{\theta}\nu_m + i\theta\theta\bar{\theta}\bar{\lambda} - i\bar{\theta}\bar{\theta}\theta\lambda + \frac{1}{2}\theta\theta\bar{\theta}\bar{\theta}D \tag{A.1.3}$$

from which follows the Abelian superfield strength

$$W_\alpha = -i\lambda_\alpha + \left[\delta^\beta_\alpha D - \frac{i}{2}(\sigma^m\bar{\sigma}^n)^\beta_\alpha(\partial_m\nu_n - \partial_n\nu_m)\right]\theta_\beta + \theta\theta\sigma^m_{\alpha\dot{\alpha}}\partial_m\bar{\lambda}^{\dot{\alpha}} \; . \tag{A.1.4}$$

D, F are auxiliary fields that can be eliminated with the equations of motion.

Identities

Making use of the non relativistic approximation $p^0 \approx m + \frac{\vec{p}^2}{2m}$, one finds

$$\sqrt{\bar{\sigma}\cdot q} \approx \frac{(\bar{\sigma}\cdot q + m)}{\sqrt{2(q^0 + m)}} \approx \frac{(\vec{\bar{\sigma}}\cdot\vec{q} + 2m + \frac{\vec{q}^2}{2m})}{2\sqrt{m}(1 + \frac{\vec{q}^2}{8m^2})} \tag{A.1.5}$$

from which follows

$$\sqrt{\bar{\sigma}\cdot q}\sqrt{\bar{\sigma}\cdot p} \approx m + \frac{1}{2}\vec{\sigma}(\vec{q}+\vec{p}) + \frac{1}{4m}\left(\frac{1}{2}(\vec{p}+\vec{q})^2 - i(\vec{p}\times\vec{q})\vec{\sigma}\right), \tag{A.1.6a}$$

$$\left(\sqrt{\bar{\sigma}\cdot q}\,\vec{\sigma}\,\sqrt{\bar{\sigma}\cdot p} + \sqrt{\sigma\cdot q}\,\vec{\bar{\sigma}}\,\sqrt{\sigma\cdot p}\right)\vec{k} \approx \vec{\sigma}\cdot(\vec{q}+\vec{p})\,\vec{\sigma}\cdot\vec{k} + 2i(\vec{p}\times\vec{k})\cdot\vec{\sigma}\,, \tag{A.1.6b}$$

$$\begin{aligned}\left(\sqrt{\bar{\sigma}_{\rm e}\cdot q}\sigma_{{\rm e}\,m}\sqrt{\bar{\sigma}_{\rm e}\cdot p}\right)\left(\sqrt{\bar{\sigma}_{\rm p}\cdot p}\sigma_{\rm p}^m\sqrt{\bar{\sigma}_{\rm p}\cdot q}\right) \approx -(\vec{q}+\vec{p})^2 - (\vec{p}-\vec{q})^2\vec{\sigma}_{\rm e}\cdot\vec{\sigma}_{\rm p} \\ - 2i(\vec{p}\times\vec{q})\cdot(\vec{\sigma}_{\rm p}-\vec{\sigma}_{\rm e}) - (\vec{p}-\vec{q})\cdot\vec{\sigma}_{\rm e}(\vec{p}-\vec{q})\cdot\vec{\sigma}_{\rm p}\,.\end{aligned} \tag{A.1.6c}$$

Another useful identity is

$$(\vec{p}+\vec{q})^2 - \frac{(\vec{p}^2-\vec{q}^2)^2}{(\vec{p}-\vec{q})^2} = 4\left(\vec{p}^2 - \frac{(\vec{p}\cdot(\vec{p}-\vec{q}))^2}{(\vec{p}-\vec{q})^2}\right). \tag{A.1.7}$$

Propagators

Propagators for gaugino, scalar and photon are given below.

$$\text{Photon:} \qquad -i\left[\frac{\eta_{mn}}{k^2+i\epsilon} - (1-\xi_\nu)\frac{k_m k_n}{k^4}\right]. \tag{A.1.8a}$$

$$\text{Gaugino:} \qquad \frac{i\not{p}}{p^2+i\epsilon}\,. \tag{A.1.8b}$$

$$\text{Scalar:} \qquad \frac{i}{p^2+i\epsilon}\,. \tag{A.1.8c}$$

$\mathfrak{so}(6)$ constants

Taken from [35] the $\mathfrak{so}(6)$ constants of the $\mathcal{N}=4$ Lagrangian are

$$\begin{aligned} c^{1ij} &= \begin{pmatrix} 0 & \sigma^1 \\ -\sigma^1 & 0 \end{pmatrix}, \qquad c^{2ij} = \begin{pmatrix} 0 & -\sigma^3 \\ \sigma^3 & 0 \end{pmatrix} \\ c^{3ij} &= \begin{pmatrix} i\sigma^2 & 0 \\ 0 & i\sigma^2 \end{pmatrix}, \qquad c^{4ij} = \begin{pmatrix} 0 & -\sigma^2 \\ -\sigma^2 & 0 \end{pmatrix} \\ c^{5ij} &= \begin{pmatrix} 0 & i \\ -i & 0 \end{pmatrix}, \qquad c^{6ij} = \begin{pmatrix} \sigma^2 & 0 \\ 0 & -\sigma^2 \end{pmatrix}. \end{aligned}$$

A.2 (BS-)Wave function and expectation values

The hydrogen bound state wavefunction is given by,

$$\begin{aligned}\psi_{nlm}(\vec{r}) = (\mu\alpha)^{\frac{3}{2}}\frac{2}{n^2}\sqrt{\frac{(n-l-1)!}{(n+l)!}}\left(\frac{2r\mu\alpha}{n}\right)^l \exp\left(-\frac{r\mu\alpha}{n}\right) \\ \cdot\,\mathrm{L}_{n-l-1}^{2l+1}\left(\frac{2r\mu\alpha}{n}\right)\cdot Y_{lm}(\theta,\phi)\,,\end{aligned} \tag{A.2.1}$$

where L and Y are the Laguerre polynomials and spherical functions. They can be called in Mathematica under LaguerreL[a,b,x] and SphericalHarmonicY[l,m,theta,phi].

Expectation values

EVs used in this thesis are

$$\langle nlm| \frac{1}{r} |nlm\rangle = \frac{\mu\alpha}{n^2} \tag{A.2.2a}$$

$$\langle nlm| \frac{1}{r^2} |nlm\rangle = \frac{(\mu\alpha)^2}{n^3(l+1/2)} \tag{A.2.2b}$$

$$\langle nlm| \frac{\vec{p}^2}{r} |nlm\rangle = \frac{(\mu\alpha)^3}{n^4}\left[\frac{2n}{l+1/2} - 1\right] \tag{A.2.2c}$$

$$\langle nlm| \vec{p}^4 |nlm\rangle = \frac{(\mu\alpha)^4}{n^4}\left[\frac{4n}{l+1/2} - 3\right] \tag{A.2.2d}$$

$$\langle nlm| \left[\frac{(\vec{r}\cdot\vec{p})^2}{r^3} + 2\pi\delta^3(\vec{r})\right] |nlm\rangle = \frac{(\mu\alpha)^3}{n^4}\left[\frac{n}{l+1/2} - 1\right] \tag{A.2.2e}$$

$$\langle n00| \pi\delta^3(\vec{r}) |n00\rangle = \frac{(\mu\alpha)^3}{n^3} \ . \tag{A.2.2f}$$

Additional EVs which are needed for spin-orbit and hyperfine structure corrections are found in [1].

A.3 Excitation of a non BPS multiplet

I am interested in how a non-BPS multiplets, the bound state of a BPS with an anti-BPS particle, transforms under $V_l \sim \mathfrak{so}(3)$ excitations, i.e.

$$V_l \otimes (\Phi_{\mathrm{e}}^{\mathrm{BPS}} \otimes \Phi_{\mathrm{p}}^{\text{Anti-BPS}}) \ . \tag{A.3.1}$$

The following analysis is for the case when the R-symmetry is $\mathfrak{so}(5)$, i.e. $\mathcal{N}=4$; in the case of $\mathcal{N}=2$, one has to replace $\mathfrak{so}(5)$ with $\mathfrak{so}(3)$ and $\mathfrak{so}(8)$ with $\mathfrak{so}(6)$ etc. The analysis for $\mathcal{N}=2$ and $\mathcal{N}=4$ is then, in principle, the same. It is useful to rewrite the creation and annihilation operator $(a^I_{a\pm}, (a^J_{b\pm})^\dagger)$ of the long multiplet with the index pair (I,a) in terms of a single index μ, running from 1 to 8 for $\mathfrak{usp}(4)_R \otimes \mathfrak{su}(2)_{little} \simeq \mathfrak{so}(5)\otimes\mathfrak{so}(3)$. After appropriate rescaling, the creation and annihilation operators satisfy the following anti commutation relations $(a^\mu_\pm \to \gamma^\mu_\pm)$

$$\{\gamma^\mu_\pm, \gamma^\nu_\pm\} = 2\delta^{\mu\nu} \ , \qquad \{\gamma^\mu_\pm, \gamma^\nu_\mp\} = 0 \ . \tag{A.3.2}$$

It is known that $\mathfrak{so}(3) \otimes \mathfrak{so}(5) \in \mathfrak{so}(8)$, where $\gamma^\mu_\pm$ is a vector in $\mathfrak{so}(8)$. The rotations of $\mathfrak{so}(8)$ $M^{\mu\nu}$ satisfy the algebra

$$[M^{\mu\nu}, M^{\rho\sigma}] = \delta^{\mu\rho}M^{\nu\sigma} - \delta^{\mu\sigma}M^{\nu\rho} - \delta^{\nu\rho}M^{\mu\sigma} + \delta^{\nu\sigma}M^{\mu\rho} \ . \tag{A.3.3a}$$

Then one can define the operators

$$S^{\mu\nu}_\pm = \frac{1}{4}[\gamma^\mu_\pm, \gamma^\nu_\pm] \tag{A.3.4}$$

which satisfy

$$[S^{\mu\nu}_\pm, \gamma^\rho_\pm] = \delta^{\mu\rho}\gamma^\nu - \delta^{\nu\rho}\gamma^\mu = [M^{\mu\nu}, \gamma^\rho_\pm] \tag{A.3.5}$$

and

$$\begin{aligned}[S_{\pm}^{\mu\nu}, S_{\pm}^{\rho\sigma}] &= \delta^{\mu\rho}S^{\nu\sigma} - \delta^{\mu\sigma}S^{\nu\rho} - \delta^{\nu\rho}S^{\mu\sigma} + \delta^{\mu\sigma}S^{\nu\rho} \\ &= [M^{\mu\nu}, S_{\pm}^{\rho\sigma}] \,.\end{aligned} \tag{A.3.6}$$

Finally, the operator

$$T^{\mu\nu} \equiv M^{\mu\nu} - S_{+}^{\mu\nu} - S_{-}^{\mu\nu} \tag{A.3.7}$$

satisfies the usual $\mathfrak{so}(8)$ commutation relations, and also commutes with $\gamma_{\pm}^{\mu}$. The algebra spanned by $\{T^{\mu\nu}, \gamma_{\pm}^{\mu}\}$ is equivalent to $\{M^{\mu\nu}, \gamma_{\pm}^{\mu}\}$. Since $\gamma_{\pm}^{\mu}$ is a representation of Φ_{BS}, one finds that it transforms trivially under a $\mathfrak{so}(3)$ V_l excitation with trivial $\mathfrak{so}(5)$ transformation.

Bibliography

[1] Christopher P Herzog and Thomas Klose. The perfect atom: bound states of supersymmetric quantum electrodynamics. *Nuclear Physics B*, 839(1):129–156, 2010.

[2] Tomas Rube and Jay G Wacker. The simplicity of perfect atoms: Degeneracies in supersymmetric hydrogen. *Journal of Mathematical Physics*, 52(6):062102, 2011.

[3] Simon Caron-Huot and Johannes M Henn. Solvable relativistic hydrogen-like system in supersymmetric yang-mills theory. *Physical review letters*, 113(16):161601, 2014.

[4] Niels Bohr. On the constitution of atoms and molecules. In *Niels Bohr, 1913-2013*, pages 13–33. Springer, 2016.

[5] Wolfgang Pauli. über das modell des wasserstoffmolekülions. *Annalen der Physik*, 373(11):177–240, 1922.

[6] E. Schrödinger. Quantisierung als Eigenwertproblem. *Annalen der Physik*, 384:361–376, 1926.

[7] P. A. M. Dirac. The Quantum Theory of the Electron. *Proceedings of the Royal Society of London Series A*, 117:610–624, February 1928.

[8] E. Fermi. Über die magnetischen Momente der Atomkerne. *Zeitschrift fur Physik*, 60:320–333, May 1930.

[9] W. E. Lamb and R. C. Retherford. Fine Structure of the Hydrogen Atom by a Microwave Method. *Physical Review*, 72:241–243, August 1947.

[10] Hans A Bethe. The electromagnetic shift of energy levels. *Physical Review*, 72(4):339, 1947.

[11] Michael I Eides, Howard Grotch, and Valery A Shelyuto. Theory of light hydrogenlike atoms. *Physics Reports*, 342(2):63–261, 2001.

[12] Morad Aaboud et al. Search for new phenomena in a lepton plus high jet multiplicity final state with the ATLAS experiment using $\sqrt{s} = 13$ Tev proton-proton collision data. 2017.

[13] Wilfried Buchmüller, ST Love, and Roberto D Peccei. Supersymmetric bound states. *Nuclear Physics B*, 204(3):429–450, 1982.

[14] P. Di Vecchia and V. Schuchhardt. $\mathcal{N} = 1$ and $\mathcal{N} = 2$ Supersymmetric Positronium. *Phys. Lett.*, B155:427–431, 1985.

[15] Juan Maldacena. The large-n limit of superconformal field theories and supergravity. *International journal of theoretical physics*, 38(4):1113–1133, 1999.

[16] Sakata Yusuke, Robin Schneider, Yuji Tachikawa, and Takemasa Yamaura. to be published.

[17] Julius Wess and Jonathan Bagger. *Supersymmetry and supergravity*. Princeton university press, 1992.

[18] Myron Bander and Claude Itzykson. Group theory and the hydrogen atom (i). *Reviews of modern Physics*, 38(2):330, 1966.

[19] Jun John Sakurai and Jim Napolitano. *Modern quantum mechanics*. Addison-Wesley, 2011.

[20] Michael Peskin and Dan Schroeder. An introduction to quantum field theory. 1995.

[21] I Lindgren. Gauge dependence of interelectronic potentials. *Journal of Physics B: Atomic, Molecular and Optical Physics*, 23(7):1085, 1990.

[22] Gregory Breit. The effect of retardation on the interaction of two electrons. *Physical Review*, 34(4):553, 1929.

[23] WA Barker and FN Glover. Reduction of relativistic two-particle wave equations to approximate forms. iii. *Physical Review*, 99(1):317, 1955.

[24] Claude Itzykson and Jean-Bernard Zuber. *Quantum field theory*. Courier Corporation, 2006.

[25] Siavosh R Behbahani, Martin Jankowiak, Tomas Rube, and Jay G Wacker. Nearly supersymmetric dark atoms. *Advances in High Energy Physics*, 2011, 2011.

[26] Julian Schwinger. Coulomb green's function. *Journal of Mathematical Physics*, 5(11):1606–1608, 1964.

[27] Tomas Rube and Jay G. Wacker. The Simplicity of Perfect Atoms: Degeneracies in Supersymmetric Hydrogen. *J. Math. Phys.*, 52:062102, 2011.

[28] Aleksey Cherman, Sašo Grozdanov, and Edward Hardy. Searching for fermi surfaces in super-qed. *arXiv preprint arXiv:1308.0335*, 2013.

[29] P Di Vecchia and V Schuchhardt. N= 1 and n= 2 supersymmetric positronium. *Physics Letters B*, 155(5):427–431, 1985.

[30] J. M. Drummond, J. Henn, G. P. Korchemsky, and E. Sokatchev. Dual superconformal symmetry of scattering amplitudes in N=4 super-Yang-Mills theory. *Nuclear Physics B*, 828:317–374, March 2010.

[31] Luis F. Alday, Johannes M. Henn, Jan Plefka, and Theodor Schuster. Scattering into the Fifth Dimension of $\mathcal{N} = 4$ Super Yang-Mills. *JHEP*, 01:077, 2010.

[32] Simon Caron-Huot and Donal O'Connell. Spinor Helicity and Dual Conformal Symmetry in Ten Dimensions. *JHEP*, 08:014, 2011.

[33] Tristan Dennen and Yu-tin Huang. Dual Conformal Properties of Six-Dimensional Maximal Super Yang-Mills Amplitudes. *JHEP*, 01:140, 2011.

[34] Jan Plefka, Theodor Schuster, and Valentin Verschinin. From Six to Four and More: Massless and Massive Maximal Super Yang-Mills Amplitudes in 6D and 4D and Their Hidden Symmetries. *JHEP*, 01:098, 2015.

[35] Ferdinando Gliozzi, Joel Scherk, and Dl Olive. Supersymmetry, supergravity theories and the dual spinor model. *Nuclear Physics B*, 122(2):253–290, 1977.

[36] Lars Brink, John H Schwarz, and Joel Scherk. Supersymmetric yang-mills theories. *Nuclear Physics B*, 121(1):77–92, 1977.

[37] R Grimm, M Sohnius, and J Wess. Extended supersymmetry and gauge theories. *Nuclear Physics B*, 133(2):275–284, 1978.

[38] J Strathdee. Extended poincare supersymmetry. *International Journal of Modern Physics A*, 2(01):273–300, 1987.

[39] W. Nahm. Supersymmetries and Their Representations. *Nucl. Phys.*, B135:149, 1978.

[40] Hans A. Bethe and Roman Jackiw. *Intermediate Quantum Mechanics*. Addison-Wesley, 3rd edition, 1997.

[41] M Veltman et al. Regularization and renormalization of gauge fields. *Nuclear Physics B*, 44(1):189–213, 1972.

[42] M Veltman et al. Scalar one-loop integrals. *Nuclear Physics B*, 153:365–401, 1979.

[43] Michael I Eides. Weak-interaction contributions to hyperfine splitting and lamb shift. *Physical Review A*, 53(5):2953, 1996.

[44] William E Caswell and G Peter Lepage. Effective lagrangians for bound state problems in qed, qcd, and other field theories. *Physics Letters B*, 167(4):437–442, 1986.

[45] Patrick Labelle and S. Mohammad Zebarjad. Derivation of the Lamb shift using an effective field theory. *Can. J. Phys.*, 77:267–278, 1999.

[46] Antonio Pineda and Joan Soto. The lamb shift in dimensional regularisation. *Physics Letters B*, 420(3):391–396, 1998.

[47] Antonio Pineda. The Static potential in N = 4 supersymmetric Yang-Mills at weak coupling. *Phys. Rev.*, D77:021701, 2008.